Studies on Regulation of Transglutaminase 2 in Hypoxia Driven Chronic Kidney Disease

A thesis submitted during 2021 to the University of Hyderabad
In partial fulfillment of the award of a Ph.D. degree in the
Department of Biochemistry, School of Life Sciences

By

Kolligundla Lakshmi Prasanna
Reg. No. 15LBPH12

Department of Biochemistry
School of Life Sciences
University of Hyderabad
Hyderabad
INDIA

August 2021

University of Hyderabad, Hyderabad- 500 046, India

CERTIFICATE
(For Ph.D Dissertation)

This is to certify that the thesis entitled "**Studies on Regulation of Transglutaminase 2 in Hypoxia Driven Chronic Kidney Disease**", submitted by **Kolligundla Lakshmi Prasanna**, bearing Reg. No. **15LBPH12** in partial fulfillment of the requirements for the award of Ph.D. in Biochemistry is a bona fide work carried out by her under my supervision and guidance.

This thesis is free from plagiarism and has not been submitted previously in part or in full to this or any other university or institution for award of any degree or diploma.

A. Publications:

1. Singh AK*, Kolligundla LP* et al., Detrimental effects of hypoxia on glomerular podocytes. JPB, 2021. DOI-10.1007/s13105-021-00788 (*Equal contribution).
2. Nakuluri K, Nishad R, Mukhi D, Kumar S, Nakka P.V, Kolligundla LP et al., Cerebral ischemia induces TRPC6 via HIF1alpha/ZEB2 axis in the glomerular podocytes and contributes to proteinuria. Sci Rep, 2019. 9(1): p.17897.

B. Conferences:

1. National Workshop on "Molecular Docking Studies in Drug Discovery" from 29th to 31st, May 2019 at Kakatiya University, Warangal, Telangana, India.
2. "85th Annual Meeting of Society of Biological Chemists" from 21st to 24th November, 2016 at CSIR- Central Food Technological Research Institute, Mysuru, India.
3. International Conference on "Structure Based Drug Designing and Applications to Infectious Diseases" from 1st to 5th February, 2016 at IIIT Hyderabad, India.

Further, the student has passed the following courses towards fulfillment of coursework requirement for Ph.D. degree.

Course code	Name of the Course	Credits	Result
BC 801	Analytical Techniques	4	Pass
BC 802	Research ethics, Data analysis and Biostatistics	3	Pass
BC 803	Lab Work & Seminar	5	Pass

P. Anil Kumar
Supervisor

Dr. P. ANIL KUMAR
Assistant Professor
Department of Biochemistry
University of Hyderabad
Hyderabad-500 046. India.

Head of the Department

HEAD
Dept. of Biochemistry
SCHOOL OF LIFE SCIENCES
UNIVERSITY OF HYDERABAD
HYDERABAD-500 046.

Dean of the School

DEAN
School of Life Sciences
University of Hyderabad
Hyderabad - 500 046.

University of Hyderabad, Hyderabad- 500 046, India

CERTIFICATE

This is to certify that the thesis entitled "**Studies on Regulation of Transglutaminase 2 in Hypoxia Driven Chronic Kidney Disease**", submitted by **Kolligundla Lakshmi Prasanna**, bearing Reg. No **15LBPH12** in partial fulfillment of the requirements for the award of Doctor of Philosophy in Biochemistry is a bonafide work carried out by her under my supervision and guidance.

The thesis has not been submitted previously in part or in full to this or any other University or Institution for the award of any degree or diploma.

P. Anil Kumar
Signature of the Supervisor

Dr. P. ANIL KUMAR
Assistant Professor
Department of Biochemistry
University of Hyderabad
Hyderabad-500 046. India.

Head of the Department

HEAD
Dept. of Biochemistry
SCHOOL OF LIFE SCIENCES
UNIVERSITY OF HYDERABAD
HYDERABAD-500 046.

Dean of the School

DEAN
School of Life Sciences
University of Hyderabad
Hyderabad - 500 046.

University of Hyderabad
Hyderabad – 500 046, India

DECLARATION

I, **Kolligundla Lakshmi Prasanna,** hereby declare that this thesis entitled "**Studies on Regulation of Transglutaminase 2 in Hypoxia Driven Chronic Kidney Disease**", submitted by me under the supervision of **Dr. Anil Kumar Pasupulati**, and is a bonafide research work. I also declare that it has not been submitted previously in part or in full to this University or any other University or Institution for the award of any degree or diploma.

Date: 09-08-2021

K. Lakshmi Prasanna
Signature of Student
(Reg. No. 15LBPH12)

P. Anil Kumar
Signature of Supervisor

Dr. P. ANIL KUMAR
Assistant Professor
Department of Biochemistry
University of Hyderabad
Hyderabad-500 046. India.

Acknowledgments:

I want to express my sincere gratitude to my supervisor, Dr. P. Anil Kumar, for his constant guidance throughout my Ph.D.

I want to thank doctoral Committee Members Prof. Ravi Gutti and Dr. Santosh Kumar Padhi for their semester evaluations and suggestions.

I want to thank Prof. S. Rajagopal, Dr. A. Bindhu Madhav Reddy for their valuable suggestions.

Further, I would like to thank all my teachers and non-teaching faculty of the Department of Biochemistry.

I thank Dr. C.S. Srinivas Rao sir from Dhanush academy Kurnool who actually helped me get a seat in UOH for my master's.

I want to thank all my lab mates, Dr. Sandeep, Ashish, Sumati, Rajesh, Abrar, Aiswarya, Praneeth killaka and Prathyusha for providing a good atmosphere to work in the lab. I thank my formal lab members Dr. Krishna Murthy and Dr. Dhanunjay Mukhi, Dr. Rajkishor Nishad.

I want to thank my parents and in-laws for their support, encouragement, and patience.

I am thankful to my SLS friends Samriddhi, Arpita, Ram Gopal Reddy for their help in doing experiments.

I thank my non-SLS friends Surendra, Aruna, Hasini and Naresh for their moral support and care about me.

I thank the NFHEST fellowship for sanctioning fellowship during my study and DST-SERB, LSRB, DHR, ICMR, STARS, and DRDO for providing the funding for the laboratory.

Abbreviations:

2-APB, 2-aminoethoxydiphenyl borate

bHLH, basic-Helix-Loop-Helix

BTPDM1, Benzothienylpyridine Dimethylamine

CBZ, Carbobenzyloxy-L-Glutaminylglycine

ChIP, Chromatin Immunoprecipitation

CKD, Chronic Kidney Disease

C-TAD, C-Terminal Transactivation Domain

CTGF, Connective Tissue Growth Factor

CXCR4, chemokine receptor type 4

DCT, Distal Convoluted Tubule

DKD, Diabetic Kidney Disease

DMSO, Dimethylsulfoxide

DN, Diabetic Nephropathy

ECM, Extra Cellular Matrix

EPO, Erythropoietin

ESKD, End-Stage kidney Disease

FAK, Focal Adhesion Kinase

FG4592, Roxadustat

FPE, Foot Processes Effacement

FSGS, Focal Segmental Glomerulosclerosis

GBM, Glomerular Basement Membrane

GDP, Guanosine diphosphate

GFB, Glomerular Filtration Barrier

GFR, Glomerular Filtration Rate

GTP, Guanosine Triphosphate

HIF, Hypoxia-Inducible Factor

HREs, Hypoxia-Responsive Elements

ID, Inhibitory Domain

MCAO, middle cerebral artery occlusion

MCD, Minimal Change Disease

MEA, 2-mercaptoethylamine

MET, Mesenchymal to Epithelial Transdifferentiation

MMPs, Matrix Metalloproteinases

NLS, Nuclear Localization Sequence

ODD, Oxygen-Dependent degradation Domain

PAI1, Plasminogen Activator Inhibitor1

PCR, Polymerase Chain Reaction

PCT, Proximal Convoluted Tubule

PHD, Prolyl Hydroxylase

pVHL, Von Hippel–Lindau tumour suppressor

RAS, Renin-Angiotensin-Aldosterone System

Rg, Radius of gyration

RMSD, Root Mean Square Deviation

RMSF, Root Mean Square Fluctuation

SD, Slit Diaphragm

siRNA, Small interfering RNA

siTRPC6, small interfering Transient receptor potential cation channel C6

SPCE model, extended simple point charge model

TAD, Terminal transactivation Domain

TGM2, Transglutaminase 2

TIMP, Tissue inhibitors of matrix metalloproteinase

TRPC6, Transient Receptor Potential Channel 6

UACR, Urine Albumin to Creatinine Ratio

VEGF, Vascular Endothelial Growth Factor

ZEB2, Zinc-finger E-Box-homeobox 2

Table of contents:

Contents of Figures and Tables:

1. Introduction

1.1. Structure and function of Kidney:

Kidneys are the predominant excretory organs that lie retroperitoneally (behind the peritoneum) in the abdomen, either side of the vertebral column. The function of the kidneys is attributed to its smallest functional unit, the nephron. The human kidney is made up of approximately two million nephrons. The structure of the nephron was provided in **Figure 1**. A nephron consists of two regions: glomerulus and renal tubule. The glomerulus is responsible for filtering small molecules and water from the blood to form primary urine, whereas the tubular system ensures selective reabsorption and secretion. Thus, both glomerulus and tubule contribute to the final composition of urine. The tubule includes the proximal (PCT) and distal tangled tubules (DCT), connected by Henle's loop, which converges into a collecting tube. There are structures like pyramids called Bartolini pyramids in the kidney, consisting of several renal tubules and collecting ducts. Each pyramid's base connects to the renal hilum, which collects urine and transports it to the urinary bladder.

The vertebrate kidney is essential in preserving homeostasis by coordinating the water balance, electrolyte balance, blood pressure, and ensuring excretion of ultra-filtrated urine [1]. Kidneys secrete erythropoietin and renin, thereby regulating the synthesis of red blood cells and blood pressure via renin-angiotensin-aldosterone system (RAS) respectively. Kidneys also regulate the metabolism of calcitriol, an active form of vitamin D [2]. In healthy conditions, kidneys rigorously regulate the concentration of proteins in the urine by ensuring ultrafiltration of glomerular filtrate and selective reabsorption [1]. Since albuminuria is the known marker for examining the renal condition, urinary protein concentration is measured by the albumin levels in 24 hours. Urinary excretion of varying

degrees of serum albumin is a well-known predictor of renal outcome [3]. Micro-albuminuria (30 to 300 mg/24 h) followed by macro-albuminuria (≥300 mg/24 h) over months to years indicate progressive renal function loss. A panoply of cellular and molecular factors contributes to pathological proteinuria [4]. Clinical conditions, including preeclampsia, diabetes mellitus, cardiovascular disease, and hypertension, could provoke proteinuria [5]. Proteinuria for an extended period is referred to as chronic kidney disease (CKD), and the condition, if left untreated, often progresses to end-stage kidney disease (ESKD) [6]. Glomerular diseases account for most CKD, which eventually goes to ESKD [7]. CKD affects about one in every ten people in the USA, and patients with CKD have a 3 to 5-fold increased risk of mortality [8]. The progressive character of CKD is linked to ongoing tissue loss and replacement by extracellular matrix (ECM), which leads to renal fibrosis. Although ECM provides structural and biological support to neighboring cells, uncontrolled accumulation and excess deposition of ECM protein lead to the progressive loss of kidney architecture and compliance.

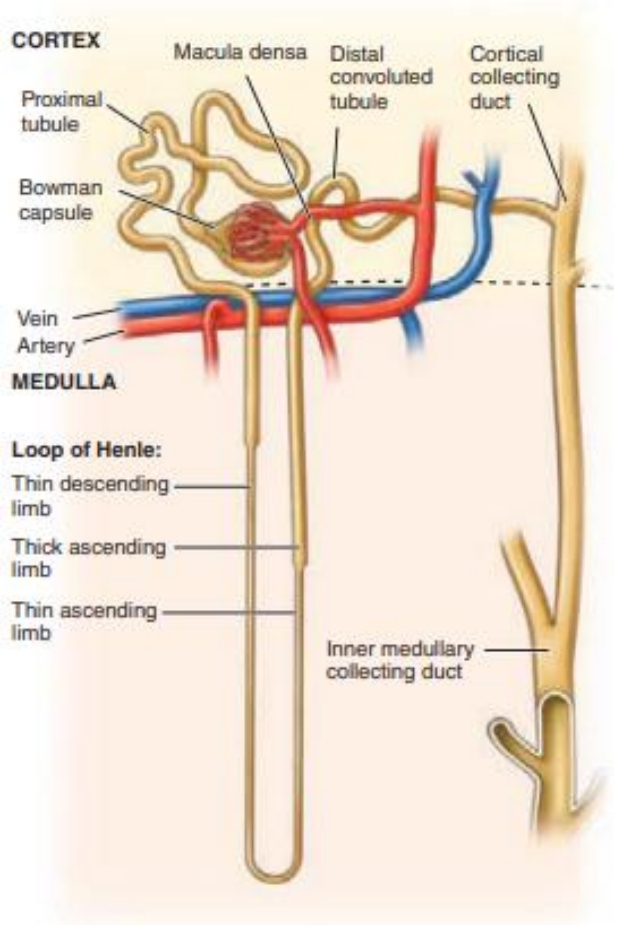

Figure 1. Structure of human nephron. The blood is filtered in the glomerulus that is mainly concentrated in the cortex part of kidney. Whereas, medulla contains the tubule part which only participate in electrolyte and water reabsorption. Tubular part works against gradient across various segments. Collecting duct collects the concentrated urine and send it to the renal pelvis.
(Source: Harrison principles of internal medicine, Edition 19, Page. 332e-5).

1.2 Glomerulus and Glomerular Filtration Barrier:

The glomerulus is a bunch of specialized renal capillaries lined with endothelial cells and covered by a glomerular basement membrane (GBM). Podocytes, a specialized visceral cells provide epithelial coverage to the capillaries and in turn to GBM. Together, endothelial cells, GBM, and podocytes form a size, shape, and charge selective glomerular filtration barrier (GFB). This complex arrangement is required for the filtration of whole plasma volume continuously [9]. Glomerulus ensures the size, shape, and charge selective filtration of blood components. This permselectivity is contributed by a three-layered GFB that allows the filtration of molecules smaller than 60 kDa [10]. The loss of protein in the urine during an early proteinuric kidney disease features indicates damage to the GFB [11]. Endothelial cells are 70-100 nm thick and cover up to half of the volume of the entire glomerular surface area. The GBM is 250-300 nm thick. It comprises extracellular components such as fibronectin, collagen, vimentin, α-smooth actin and glycosamine glycans, heparin sulfate, and chondroitin sulfate proteoglycans. The podocytes are terminally differentiated visceral epithelial cells with primary and secondary foot processes that enwrap the capillaries to provide epithelial coverage [12]. Besides being a critical player in attributing glomerular perm selectivity, podocytes seek greater attention as they account for

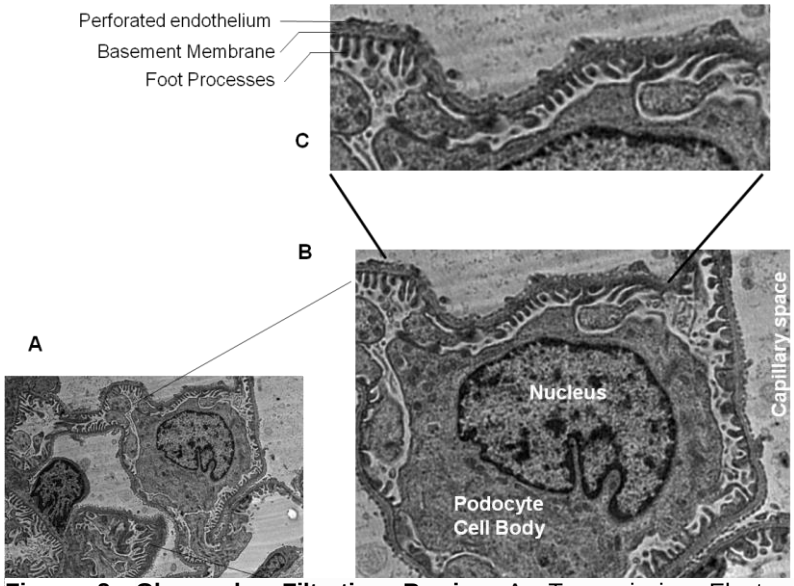

Figure 2. Glomerular Filtration Barrier. A. Transmission Electron Micrograph of the podocyte, major processes, and foot processes (Scale-2 µm). B. Morphology of an individual podocyte with enlarged nucleus C. The three anatomic layers of glomerular filtration apparatus: perforated endothelium, basement membrane, and foot processes of podocyte.

more than 30% of glomerular cells. In normal healthy conditions, filtration by GFB is regulated tightly. Any damage in the GFB leads to the appearance of proteins in the urine, called proteinuria. In GFB, podocytes are very critical and have a significant role. The damage or loss of podocytes usually correlates with proteinuria. The architecture of GFB by Transmission Electron Micrograph was shown in **Figure 2**.

1.2.1 Podocyte structure and function:

Podocytes are the terminally differentiated specialized epithelial cells with a complex cytoarchitecture. They contribute at least 40% of the core components of the GBM [13]. They consist of a vast cell body with a high nuclear-cytoplasmic ratio and foot processes (FPs) [14]. FPs help podocytes adhere firmly to the GBM and provide epithelial coverage to the glomerular capillaries. Adjacent FPs are connected with the slit-diaphragm (SD), which is the sole contact between podocytes and plays a significant role in establishing size-selective permeability of the GFB to retain proteins in the plasma while disposing small solutes into the primary filtrate.

Interestingly, SD is made up of both tight junction and adherent junction proteins [15]. The SD consists of certain extracellular domains of transmembrane proteins named podocin, nephrin, CD2AP, P-cadherin, Neph-1, etc. Podocytes oppose the glomerular hydrostatic pressure in the glomerular capillaries, which is the natural driving force that ensures macromolecular filtration [14]. The podocytes were always prone to detach from GBM and excreted through urine because they are attached to the GBM only with FPs [16]. Podocytes are frequently challenging to drugs, metabolic waste contents, and toxins that the kidney can excrete.

VEGF (vascular endothelial growth factor) synthesized by podocytes is required to maintain endothelium and ECM components of GBM. Since podocytes are instrumental for glomerular filtration, podocyte injury induces a complex set of biological responses in

the glomeruli, leading to proteinuria [17]. Glomerular diseases, such as minimal change disease (MCD), diabetic nephropathy (DN), and focal segmental glomerulosclerosis (FSGS) are presented with podocyte damage and often end up with fibrotic phenotype, which could be triggered by mesangial cell activation, ECM overproduction, and scar formation [7, 17].

The functions of podocytes are (i) to maintain the architecture of the glomerulus, (ii) to preserve the filtration unit throughout the SD, (iii) to monitor the charge & size, distinctive features of GFB, (iv) regulation of glomerular filtration rate (GFR). The podocytes also maintain the capillary wall and its loop tension. Podocyte acts as a unit for unified filtration, with a potent cross-talk among mesangial-endothelial cells and GBM. Damage to the podocytes causes flattening of the extensions of focal adhesions, and lamellipodial roots ultimately lead to foot processes effacement (FPE). According to the previous studies, FPE is the common pathway for every type of renal injury, in which reorganization cytoskeleton is most common [11].

1.2.2. GBM and Extracellular Matrix (ECM):

The GBM is a layer of ECM components present between the fenestrated endothelium and FPs of podocytes. GBM is made with highly specialized ECM components forming layers to curb the cells and connecting the cells with the interstitial matrix [18]. The ECM is an extensive network of molecules such as glycoproteins, extracellular macromolecules, hydroxyapatite, and enzymes that give structural and mechanical support, crucial for holding to neighboring cells. The GBM mainly contained type IV collagen, nidogen, laminin, and proteoglycan such as heparin sulfate. Along with those molecules, GBM also has general protein families such as collagen α3α4α5 (IV), laminin-521, and agrin. Matrix metalloproteinases (MMPs) and plasminogen/plasmin are the proteolytic enzymes that can degrade the ECM. Tissue inhibitors of matrix

metalloproteinase (TIMP) and plasminogen activator inhibitors can inhibit the proteolytic enzymes, thus help accumulate ECM. The proteolytic enzymes and their inhibitors are the primary reasons for maintaining the homeostasis of ECM. Fibrotic scars, deformities of normal renal tissue, and a reduction in healthy nephrons are symptoms of excessive ECM accumulation. Both, overproduction and accumulation of ECM proteins promote uncontrolled ECM buildup in renal fibrosis. Fibrosis is the uncontrolled accumulation and excess deposition of ECM protein that leads to the progressive loss of tissue architecture and compliance. Renal fibrosis is a well-known common mechanism that leads to the degradation of kidney tissue and renal failure in a wide range of CKDs.

1.3. Risk factors for compromised renal function:

1.3.1. Renal fibrosis and ECM Remodeling:

Fibrosis in the kidney is an inevitable consequence of failed kidney repair during chronic or sustained injury or stimulus. Kidney fibrosis, measured by the expression levels of collagen and fibronectin, does not limit the glomerular and tubular compartments but continues to expand to the entire kidney, including the renal pelvis, leading to complete shutdown of kidney function [19]. During kidney fibrosis, the collagens and fibronectins are the ECM proteins excessively produced and sometimes due to the decrease in the ECM catabolizing enzymes such as MMPs or increase of TIMPs [20]. Glomerulosclerosis is a term that nominates ECM accumulation in the glomerulus only due to structural alterations such as thickening of GBM and formation of glomerular synechiae due to the detachment of podocytes. Therefore, damage to the glomerular compartment results in the gradual loss of functional nephrons. This is particularly interesting because the nephrons' tubular structures can regenerate, but the glomerular cells, particularly, podocytes are lost once they are injured [21, 22].

While kidney fibrosis is paramount and culminates in kidney function loss in CKD or DKD, the molecular mechanisms and cell types involved in both kidney diseases are different from the animal models developed [23-25]. Several mouse and rat models were developed to study glomerular fibrosis (sclerosis) and tubular fibrosis individually to study the mechanism of fibrosis. Unilateral ureteral obstruction, folic acid injury, and repetitive doses of cisplatin or aristolochic acid can be used to study the fibrosis of kidney injury, particularly for tubular fibrosis [24, 25]. Whereas for the glomerular fibrosis, fewer models developed, such as puromycine aminonucleoside, uninephrectomy, and streptozotocin with uninephrectomy [26, 27]. Although these models can induce fibrosis and severe damage to the kidney, many underlying mechanisms were identified [28]. A body of evidence indicates that these mechanisms can converge into common pro-fibrogenic and pro-inflammatory pathways [29, 30]. Therefore, therapeutic options against fibrosis could successfully prevent kidney injury regardless of the mechanism of disease.

1.3.2. Mechanism of renal fibrosis:

Aggressive extension of the normal wound healing process culminates in tissue scarring or fibrosis. Epithelial-to-mesenchymal transition, epithelial cell injury, and inflammatory cell infiltration are the central mechanisms that interest the progression of kidney fibrosis [31]. Several immune cell types were reported to play a crucial role in the advancement of renal fibrosis, which include, fibroblasts, myofibroblasts, and epithelial cells [32]. A recent single-cell study revealed that myofibroblasts are the significant cell type responsible for ECM deposition and accumulation [33]. Although this study highlighted myofibroblasts are the primary cell type for fibrosis, these cells need a series of differentiation events that generate fully mature myofibroblasts from fibroblasts. Other cell types, including mesangial, endothelial, and epithelial cells, can transform into myofibroblast development (**Figure 3**). Therefore, predominant cells are still glomerular

and tubular epithelial cells injured during kidney injury, secrete some cytokines and growth factors. Cytokines can recruit immune cells, and growth factors can support the differentiation and proliferation of fibrotic cells during sustained damage.

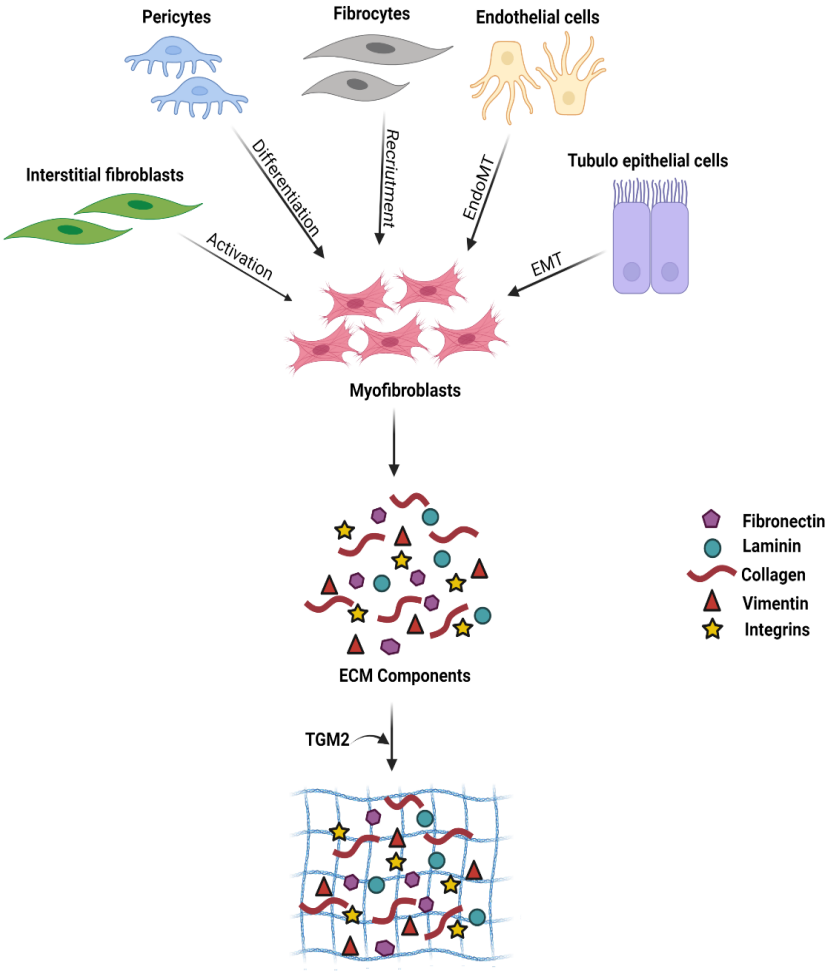

Figure 3. **Mechanism of renal fibrosis.** The myofibroblasts are the principle cells of fibrosis that originate from different sources by various mechanisms of differentiation. The myofibroblasts synthesize a huge amount of collagens, fibronectin other precursors. Upon active secretion of these ECM components are cross-linked by the TGM2 that becomes stable in disease conditions.These crosslinks cannot be reversed by any proteases in the ECM niche leading to irreversible fibrosis.

1.4. Hypoxia is the risk factor for the progression of renal fibrosis:

1.4.1. Hypoxia sensing machinery:

The hypoxia-inducible factor (HIF) pathway is the crux of oxygen sensing machinery, and the transcription factors HIF1&2 are the central molecules of this pathway. HIF1 is a heterodimer and consists of an inducible subunit HIF1α and a constitutively expressed HIF1β. HIF1α interacts with HIF1β via the shared PAS (Per-ARNT-Sim) domain [34]. The structural details of HIF1 are depicted in **Figure 4**. The basic-helix-loop-helix (bHLH) domain located at the N-terminus of both these subunits helps in DNA binding. In comparison, the C-terminal transactivation domain (C-TAD) is required to induce target gene expression [35]. The oxygen sensitivity of HIF1α is mediated by the oxygen-dependent degradation (ODD) domain, which includes two prolines (P402 and P564) and lysine (K532). Hydroxylation of prolines by iron co-factor containing prolyl hydroxylase (PHD) and acetylation of K532 by acetyltransferase (arrest-defective-1) recruit pVHL (von Hippel–Lindau tumor suppressor) [36]. The pVHL serves as a recognition molecule for the ubiquitin-protein ligase complex, which ends up targeting the HIFα subunits for ubiquitin-mediated degradation [37]. Neither hydroxylation of prolines nor acetylation of lysine occurs during hypoxia; thus, HIF1α evades ubiquitination and can dimerize with HIF1β to form HIF1. The Oxygen-dependent regulation of HIF1 is shown in **Figure 5**. Therefore, HIF1 heterodimer binds to hypoxia-responsive elements (HREs) in target gene promoters and their transcriptional enhancers that contain the core sequence (RCGTG) [38].

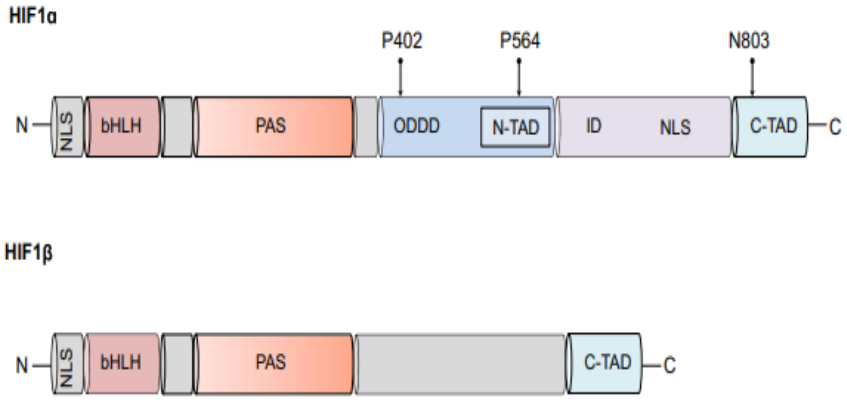

Figure 4: Structural details of HIF1α and HIF1β subunits. The N-terminal of HIF1α consists of bHLH and PAS domains. Domain bHLH is important for the heterodimerization of HIF1α with HIF1β. PAS domain helps in binding with DNA. ODD domain determines the HIF1α stability during normoxia and hypoxia. The ODD domain contains the proline residues (402&564) that are susceptible to hydroxylation during normoxia. N-TAD and C-TAD are responsible for the transcription of HIF1 target genes. The TADs are interspersed by an inhibitory domain (ID). The N-TAD overlays the ODD domain, linking the transcriptional activity of HIF1α with its stabilization. HIF1β subunit is devoid of the ODD domain, and thus it is not susceptible to degradation during normoxia.

Indeed, cooperative binding of C-TAD of HIF1α with co-activator CBP/p300 is also required for the transcriptional activation of HIF1 target genes [39]. While in normoxia, oxygen-dependent hydroxylation of asparagine (N803) residue by FIH1 (factor inhibiting HIF1), an asparaginyl hydroxylase, prevents the interaction of C-TAD with CBP/p300, thus abrogating HIF1-mediated gene transcription [40]. However, Geng et al. reported that p300 specifically acetylates HIF1α at Lys-709 and contributes to HIF1α stability, and decreases ubiquitination in normoxia and hypoxia [41]. The popular targets of HIF1 include EPO, VEGFA, PAL-1, TIMP-1, CTGF, WT1, and ZEB2 [37, 42, 43]. Besides HIF's direct gene targets, there are second-order target genes regulated by hypoxia, including gene targets of transcription factors encoded by first-order HIF1 targets, epigenetic regulators, ion-channels, and regulatory non-coding RNAs [37, 44].

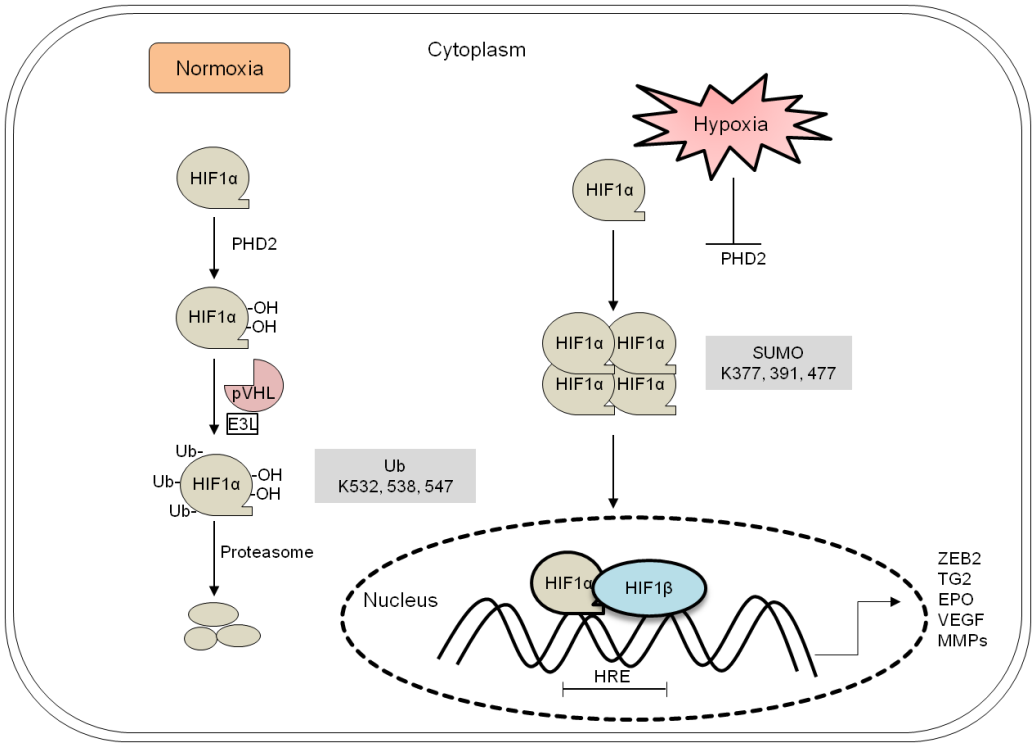

Figure 5. Oxygen-dependent regulation of HIF1 formation. HIF1α undergoes hydroxylation during normoxia by prolyl hydroxylases (PHDs) that use oxygen as a co-substrate. This hydroxylation recruits VHL protein. VHL is an E-3 ubiquitin ligase, and thus, hydroxylated HIFs undergo ubiquitination. During hypoxia, PHDs unable to hydroxylate HIF1α and facilitate HIF1α dimerization with HIF1β to form a transcriptionally active HIF1 complex. In contrast, sumoylation at lysine 377, 391, and 477 of HIF1α reduces its transcriptional activity.

1.5 Role of hypoxia in glomerular pathology:

1.5.1 Hypoxia and podocyte epithelial-to-mesenchymal transition:

Epithelial-to-mesenchymal transition (EMT) is a highly coordinated cellular event that predominantly occurs during development, wound healing, and metastasis. During this phenotypic switch, epithelial cells dedifferentiate, lose cell-cell contacts, compromise adherence nature, become motile, and acquire the ability to traverse the extracellular matrix [45]. Epithelial cell transformation to motile fibroblast-like cells is accompanied by repression of epithelial surface markers and induction of mesenchymal markers. Podocytes are originated from the metanephric mesenchyme through mesenchymal to

epithelial transdifferentiation (MET) [46]. It is now primarily considered that podocytes are visceral epithelial cells, not a typical epithelial cell, due to mesenchymal markers' expression and epithelial cell markers [47]. Because of the expression of dual-specificity markers, podocytes are at high risk of EMT occurring during injuries. EMT and detachment of podocytes from underlying GBM have been considered cellular events that contribute to loss of kidney function during glomerular diseases and DN [6]. The presence of viable podocytes in urine from experimental and clinical studies of glomerular diseases suggests detachment of intact podocytes [48, 49]. In rodents exposed to normobaric hypoxia, induction of HIF1α is accompanied by podocyte EMT [50].

It should be noted that hypoxia prevails in diabetic tissues, and elevated HIF1α was reported in biopsy sections from patients with DN and CKD [51]. ZEB2 is a predominant transcription factor that drives EMT of podocytes, being recently identified as a direct of HIF1α. Indeed, ZEB2 is associated with the EMT of podocytes in stroke-induced ischemic injury [44]. ZEB2 is the δEF1 family transcription factor with both repressor and activator functions. Induction of ZEB2 drives repression of epithelial markers (E- and P-cadherin) and expression of mesenchymal markers (e.g., N-cadherin), so-called cadherin switch, and a hallmark of EMT. As podocytes EMT manifests in a reduced number of podocytes, the residual cells can not compensate for the filtration function and eventually result in glomerular dysfunction, proteinuria, and glomerulosclerosis [17]. EMT is considered the primary mechanism of podocyte depletion and pathogenesis of DN [52]. Nevertheless, HIF1α-independent decrease in epithelial markers such as E-cadherin and kidney-specific cadherin 16 was observed [53].

1.5.2 Hypoxia and podocyte cytoskeletal rearrangements:

The cytoskeleton is essential to maintain the structure, shape, and function of podocytes. Podocyte has a unique shape, and it is crucial for its functions that are solely

supported by the dynamic reorganization of actin- cytoskeleton [54]. Chang et al. demonstrated that podocytes, when exposed to hypoxia, induced B7-1 gene expression along with HIF1α [55]. B7-1 is an essential driver of podocyte stress fiber formation. Co-expression of these two proteins is accompanied by the interaction of the cytoplasmic domain of B7-1 with the ODD domain of HIF1α, leading to the disruption of an orderly arrangement of actin fibers and increased motility of podocytes. B7-1 knockdown blunted both hypoxia-induced derangement of stress fibers and motility.

Since podocytes are motile [56], altered motility due to derangement of stress fibers could disrupt these cells' barrier function. Podocyte cytoskeleton remodeling manifests the loss of the sub-podocyte space [57]. Sub-podocyte space imparts ultrafiltration and hydraulic resistance to ensure glomerular permeability [58]. Filtration dynamics of the sub-podocyte space are expected to be altered in clinical conditions that elicit remodeling of the podocyte cytoskeleton. Furthermore, the dimensions of sub-podocyte space are affected by the foot process effacement [59]. The apical surface of podocytes facing Bowman's space possesses the negative charge of proteins such as podocalyxin and podoplanin. This surface's anionic charge maintains separation between adjacent foot processes, thus maintaining glomerular architecture and its function. Since the cell surface is associated with the actin cytoskeleton via protein-protein interactions, altered cytoskeletal interactions during hypoxia could influence the podocyte's architecture in total [60].

In a recent study, HIF1α/ZEB2 axis was shown to induce TRPC6. This cationic channel has a preference for calcium, which leads to the increased calcium influx and resultant activation of RhoA. RhoA-dependent phosphorylation of focal adhesion kinase (FAK) resulted in cytoskeletal rearrangement in podocytes when exposed to hypoxia [44]. Podocytes, in addition to providing epithelial coverage to pulsating glomerular capillaries,

apply static forces to maintain the glomerular filtration barrier by remodeling the actin-based cytoskeleton [61]. It is believed that derangement in the actin cytoskeleton and injury to focal adhesions could adversely affect podocyte shear stress and disconnect podocytes from the basement membrane. Furthermore, to sustain the complex cellular morphology and cytoskeletal dynamics, podocytes rely on a constant ATP supply. It is very well-known that during hypoxia, HIF1α shut-downs aerobic respiration and favors anaerobic glycolysis; nevertheless, how a podocyte is coping with energy needs during hypoxia remains to be explored.

1.5.3 Hypoxia and glomerulosclerosis:

Altered renal tissue oxygenation is closely associated with the development of renal fibrosis [62]. Under hypoxic conditions, HIF-1α accelerates tissue fibrosis by upregulating the profibrogenic genes such as TIMP1, CTGF, and PAI-1 [51, 63]. HIF influences most ECM genes, and their expression is correlated with glomerular fibrosis [64, 65]. Col1A2 (α2 (I) collagen), a significant component of fibrotic tissue, is under direct transcriptional control of HIF-1α [66]. HIF-1α knockout significantly reduces the development of glomerulosclerosis in the NEP25 podocyte injury model [66]. Both podocytes and tubular epithelial cells express FIH1 [67]. FIH1 disrupts the interaction between HIF1α and co-activators p300/CBP, impairing HIF1 transcriptional activity. Like PHD, FIH1 activity is also inhibited by hypoxia resulting in HIF1α stabilization [40]. FIH1 silencing in podocytes enhanced transcription of hypoxia-inducible genes in a HIF-independent manner [67]. A gradual decrease of glomerular FIH1 expression was paralleled by the induction of profibrotic molecule CXCR4 in the anti-Thy-1 rat model of glomerulonephritis [67]. Hypoxia induces transglutaminase 2 (TGM2) through a HIF1-dependent pathway [68]. TG2 is involved in fibrosis by the cross-linking of ECM components [63]. TGF-β is the master regulator of tissue fibrosis, and HIF1α was shown

to regulate TGF-β expression in many cell types. It is not known whether HIF1α induces TGF-β in podocytes.

1.6 Transglutaminase 2 and renal fibrosis:

1.6.1 Transglutaminases:

The ECM homeostasis is controlled by MMPs, TIMP, and a specialized group of enzymes that support ECM balancing called transglutaminases (TGases). TGases are a vast group of enzymes containing nine members in the family, out of eight, which actively regulate different cellular processes [69]. They are involved in the skin-barrier formation, coagulation of blood, fertilization envelope hardening, assembly of ECM [70]. The dominant role of TGases is to cross-link proteins in cellular processes ranging from tissue repair to strengthening tendons, cartilages, and the fertilization envelope [70]. The TGM2 establishes an isopeptide bonds between carboxamide group of the glutamine and amino group of lysine residue [71]. These isopeptide bonds are formed sometimes within the protein but vastly between proteins such as crosslinking of fibronectin with collagens or integrins [72]. TGases are conserved from microorganisms to humans. Vertebrate TGases are calcium-dependent enzymes [73]. Interestingly, several ECM proteins (e.g., collagen) are substrates of TGM2 [70, 74, 75]. Nevertheless, TGM2 could be a therapeutic target to combat fibrotic diseases, including kidney fibrosis; therefore, understanding the mechanism of TGM2 regulation is of great importance.

Table 1: Transglutaminase family members and their expression localization and function.

Protein	Other name	MW	Localisation of the protein	Expressed in	Function
TGM1	TGK	90	Membrane, cytosolic	brain and Keratinocytes	Formation of Cell-envelope
TGM2	Tissue TG	80	Ubiquitous	Ubiquitous	Multiple
TGM3	Epidermal TG	77	Cytosolic	Squamous epithelium, brain	Formation of cell-envelope
TGM4	Prostate TG	77	Unknown	prostate	Condensation of semen
TGM5	TGX	81	Unknown	Ubiquitously expressed but not in CNS and lymph tissue	Unknown
TGM6	TGY	Unknown	Unknown	Unknown	Unknown
TGM7	TGZ	81	Unknown	Ubiquitous	Unknown
Band 4.2	ATP-binding erythrocyte membrane protein band 4.2	72	Membrane	Bone marrow, fetal liver and RBCs	Skeletal membrane component
Factor XIIIA	Fibrin-stabilizing factor	83	Cytosolic, extracellular	Astrocytes, dermal dendritic cells, chondrocytes, Platelets, plasma, synovial fluid placenta	Coagulation of blood

1.6.2.1 Structure and functions of TGM2:

Transglutaminase 2 (known as tissue transglutaminase) is an extracellular calcium-dependent transferase enzyme (EC: 2.3.2.13) [76]. Besides present in the nucleus, TGM2 is also localized to plasma membrane, cytosol, and importantly it secreted into extracellular space [77]. Calcium allosterically regulates TGM2 activity. Since low

calcium levels and high GTP levels in the cytosol, the TGM2 will be predominantly inactive under normal situations.

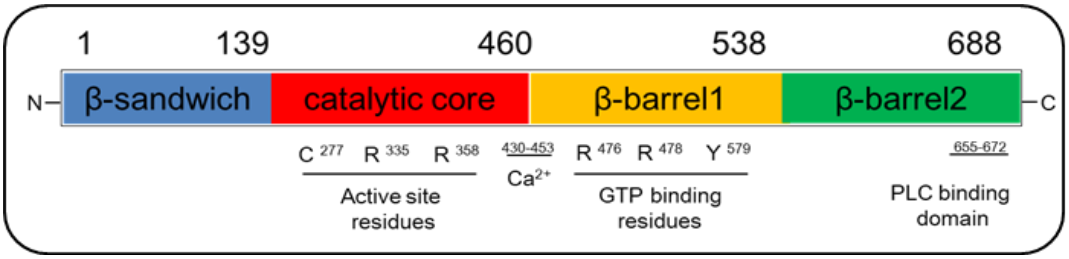

Figure 6. Structure of TGM2. The four structural domains are indicated by different color: Blue for the β-sandwich, red for catalytic core, yellow for β-barrel1 and green for β-barrel2 domain.

Human TGM2 is 76 KDa protein and consists of 686 amino acids. TGM2 is a ubiquitous member of the TGM family, and it has the ability to hydrolyze both GTP & ATP. Calcium allosterically activates TGM2 while GTP allosterically deactivates it. [78]. Crystal structure of TGM2 in a complex with an inhibitor at 2-Å resolution (PDB ID: 2Q3Z) revealed that TGM2 has four distinct domains; N-terminal β-sandwich (1-139), catalytic core (140-454), and couple of C-terminal β-barrel domains (479-585 & 586-687) are connected by the loop (455-478) [79]. The catalytic core of TGM2 comprises the residues of Cys277, His335, and Asp358 (the catalytic triad) and a conserved tryp241. The structure of TGM2 was shown in **Figure 6**. TGM2 exists in two states: open or active; and closed or inactive, which are controlled by calcium and guanosine nucleotide-binding, respectively [80, 81]. The catalytic domain and C-terminal β-barrels interact heavily in closed conformation (GTP bound), limiting access to catalytic site [81]. In contrast, calcium-binding (open) conformation pushes the β-barrels apart and let the catalytic site exposed. During Ping-Pong reaction catalyzed by TGM2, when an active site residue Cys277 attacks the substrate particularly an acyl-donor e.g., glutamine, ammonia will be released. Then, nucleophilic attack on an acyl-acceptor substrate (e.g., lysine) helps to

regenerate free enzyme, which releases an iso-peptide product, which delaminates the glutamine. The iso-peptide cross-linking mechanism by TGM2 was shown in **Figure 7**.

The proprietary nature of forming the iso-peptide bond between ECM components, TGM2, is implicated in the pathogenesis of several disorders, such as neurodegenerative disorders, Huntington's disease, diabetes, liver cirrhosis, pulmonary fibrosis, and CKD [76, 82]. A body of evidence indicates that TGM2 expression is highly increased in melanoma and glioblastoma cancer conditions. Exalted expression of TGM2 is also reported to be correlated with chemotherapeutic resistance of pulmonary and breast cancer [83]. It is noteworthy that Huntington protein, polyglutamine repeats, and α-synuclein, which form aggregates in neurodegenrative diseases are the substrates for TGM2. TGM2 can also affect cell-cell communications and cell signaling by integrins and seven transmembrane-containing receptors [84]. TGM2 has been shown to involve in cell-mediated and antibody-dependent immune responses [82].

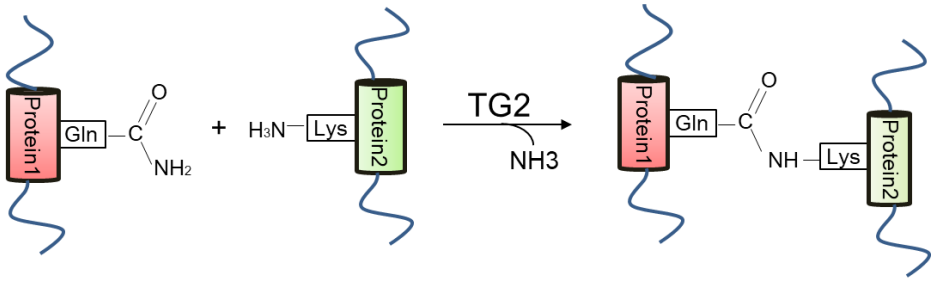

Figure 7: Cross linking activity of TGM2. The crosslinking reaction of TGM2 involves the isopeptide bond between glutamine and lysine of two proteins.

Table 2: Substrates of TGM2

S.No	Substrate for TGM2	TGM2 Localization	The Amino acid which is involved	Role in the disease condition
1.	*α*B crystalline	Intracellular	Lysine	Protein stabilization
2.	Crystalline (*β*A3, *β*B3, *β*Bp)	Intracellular	Glutamine	Protein stabilization
3.	Fibronectin	Extracellular	Glutamine	ECM interaction & stabilization
4.	Fibrinogen A alpha	Extracellular	lysine and Glutamine	ECM interaction & stabilization, inflammatory diseases
5.	Glutathione S-transferase	Intracellular	Lysine, Glutamine, and fluorescein	ECM interaction and stabilization
6.	Microtubule-associated protein tau-isoform Tau-F (Tau-4)	Intracellular	lysine and Glutamine	Neurological diseases
7.	Nidogen	Extracellular	Glutamine	ECM interaction and stabilization
8.	Osteonectin & Osteopontin	Extracellular	Glutamine	Autoimmune and inflammatory diseases

1.6.2.2 Regulation of TGM2 expression and activity:

TGM2 is broadly distributed in the cell's nucleus, cytosol, plasma membrane, and ECM [70]. Therefore, TGM2 is detected in both cytosolic, ribosomal, and nuclear fractions in cell fractionation studies. It was reported that nuclear translocation of TGM2 by importin-3 in cells undergoing apoptosis suggesting that TGM2 could be associated with cell death signaling. In the cell, relative calcium concentrations can facilitate TGM2 mediated posttranslational modifications and are essential for forming pro-

peptides and growth factors [79]. TGM2 can bind to guanosine triphosphate (GTP) and hydrolyze. Therefore, TGM2 can involve in G-protein coupled receptor signaling [85, 86]. Beta-adrenergic receptors, thromboxane, and oxytocin receptors utilize G-protein coupled signaling, enhancing TGM2 activity by increasing intracellular calcium levels [84].

1.6.2.3 Inhibitors of TGM2:

With the range of pathologies in which catalytic activity of TGM2 is implicated, including CKD, there is an urgent need for potent TGM2 specific inhibitors. Several investigators developed irreversible inhibitors such as halomethyl carbonyls, 3-Halo-4, 5-dihydroisoxazole, and competitive inhibitors resembling acyl-donor substrate tested *in vitro* and *in vivo* models. Cystamine is a competitive inhibitor of TGM2. Indeed, reducing cystamine to cysteamine or 2-mercaptoethylamine (MEA) can inhibit TGM2 competitively [87]. There are pieces of evidence that cystamine can irreversibly inhibit TGM2 at a longer incubation time [71]. This irreversible inhibition could be by forming disulfides between cysteamine and the cysteine residue present in the active site of TGM2 [71, 88]. However, cysteamine, on the other hand, has been found to have off-target effects on the protease caspase3 and to produce an increase in glutathione production. [89]. Inhibition of TGM2 activity can be achieved by employing reversible inhibitors that abolishes access of active site to substrates, which can be done without modifying the enzyme's property.

TGM2 cofactors, GTP & GDP, can execute both reversible and allosteric inhibition [90]. Analogs of GTP, such as GTPγS & GMP-PCP, were showed to inhibit TGM2 activity reversibly. Divalent cations such as Zn2+ can reversibly inhibit TGM2 activity by replacing Ca2+ from the metal-binding site of the enzyme [71, 91]. In an inhibitor screening library, few chemical compounds reacted with TGM2 with slow binding kinetics but specific to TGM2. Irreversible inhibitors have also been developed for TGM2, including carbobenzyloxy-L-glutaminylglycine (CBZ), 3-halo-4,5-dihydroisoxazoles, gluten

peptides, and iodoacetamide [82]. CBZ has been widely used to study the enzymatic activity of TGM2 in *in vitro* systems. Idoacetamide forms a strong thioether bond with cysteine residues of TGM2 and irreversibly inactivates TGM2. Since iodoacetamide is a small molecule, it has a non-specific interaction with cysteine residues of TGM2 away from the active site. Nevertheless, there have no specific inhibitors been developed for TGM2 for human trials. Regardless, a clinically validated TGM2 inhibitor is yet to be obtained for human use.

1.7 Hypothesis:

TGM2 is considered a therapeutic target to combat fibrotic diseases, including kidney fibrosis and CKD [92]. Understanding the mechanism of TGM2 regulation is of great importance. Hypoxia is the predominant stimuli that provoke renal injury and fibrosis, whereas HIF1α, but not other HIFs, significantly transduces the cellular effects of hypoxia. Since elevated expression of TGM2 was observed in CKD, where hypoxia is a dominant factor, we hypothesize that HIF1α could elicit glomerular manifestations via regulating TGM2 expression and activity. A recent study from our group established that HIF1α induces ZEB2 in podocytes and subsequent podocyte injury and proteinuria in ischemic rats [44]. The mechanism of HIF1α dependent TGM2 and glomerulosclerosis is investigated with the following objectives.

Objectives:

- Does HIF1α induced ZEB2 regulate TGM2 expression in glomerular podocytes?
- Does inhibition of HIF1α accumulation prevent TGM2 dependent adverse effects on glomerular biology?
- We are designing and validating the inhibitors against TGM2 to combat renal fibrosis.

2. Results

2.1 ZEB2/TRPC6 axis transduce HIF1α dependent regulation of TGM2 in glomerular podocytes

2.1.1 Abstract:

Glomerular podocytes are instrumental in ensuring glomerular permselectivity and regulating the integrity of glomerular biology. Podocytes are vulnerable to noxious stimuli such as hypoxia, and podocyte injury progresses to glomerulosclerosis and impaired kidney function. The mechanism of hypoxia-induced podocyte injury vis-a-vis glomerulosclerosis has remained enigmatic. Hypoxia-inducible factor 1α, which transduces hypoxic adaptations, induces TGM2, a calcium-relying enzyme that catalyzes the intra-molecular ε-(γ-glutamyl) lysine cross-links of ECM molecules and implicates in fibrosis. In this study, we explored the regulatory mechanism of TGM2 by HIF1α. Stabilization of HIF1α by FG4592 (Roxadustat), leading to the increased ZEB2 expression and its downstream target TRPC6. ZEB2 transcriptionally activates TGM2 expression, whereas, via TRPC6, it induces calcium influx, thus increase TGM2 activity. Blocking the TRPC6 action or suppressing its expression only partially attenuated FG4592 induced TGM2 activity, whereas suppression of ZEB2 expression significantly abolished TGM2 activity. This study demonstrates that stabilization of HIF1α stimulates both TGM2 expression and activity, whereas abrogation of HIF1α by metformin prevented HIF1α regulated TGM2 and consequent glomerular injury.

2.1.2 Introduction:

Glomerular diseases are devastating, and the consequence is massive proteinuria frequently leads to CKD, which eventually progresses to ESKF [7]. CKD is linked to continual tissue loss, ultimately replaced by ECM, resulting in renal fibrosis. Even though ECM provides mechanical and biological support to the surrounding cells, undisciplined accumulation and excess deposition of ECM protein lead to the progressive loss of kidney architecture and consent.

The TGM2 enabled ε (γ-glutamyl) lysine iso-peptide cross-linking facilitates inappropriate deposition of ECM proteins and is resistant to proteolytic degradation [73]. Several ECM proteins (eg: Collagen) are substrates of TGM2 [74]. Although TGM2 is implicated in scarring of the liver [93] and lung [94], the enzyme has been widely explored in kidney fibrosis [95]. A strong association between TGM2 levels (R2 = 0.92), ε (γ-glutamyl) lysine iso-peptide cross-linking (R2 = 0.86), and the advancement in scarring of tissue were reported in the early 20th century, suggesting that there is a lot to understand its role in the kidney diseases [95]. Since TGM2 is considered a therapeutic target to combat fibrotic diseases, including kidney fibrosis and CKD, understanding the mechanism of TGM2 regulation is of great importance. Hypoxia is among several noxious stimuli that provoke tissue injury and fibrosis, and HIF1α transduces the cellular effects of hypoxia. This chapter investigated the mechanism of regulation of TGM2 in the settings of elevated HIF1α and found that HIF1α /ZEB2 axis control both TGM2 expression and activity.

2.1.3 Materials & Methodology

2.1.3.1 Reagents and Materials: The primary antibodies are as following: Fibronectin (#PAA037) and Vimentin (#PAB040) antibodies were procured from Cloud-clone Technologies. α-SMA (#19245), β-Actin (# 4970), N-Cadherin (#13116), and E-cadherin (#3195) were acquired from CST. TGM2 (NBP2-54633), HIF-1α (NB100-105), and ZEB2 (NBP1-82991) antibodies were purchased from Novus Biologicals. Anti-TRPC6 (#PA5-20256) antibody and Alexa Fluor® 555 streptavidin were obtained from Thermo. Florescence-based Alexa labeled secondary antibodies were obtained from Vector Labs. Secondary antibodies were procured from Jackson Laboratories. Nitrocellulose membrane (#10600001) from GE healthcare. Protein marker and ECL reagent was purchased from Bio-Rad Laboratories. RPMI 1640 media (#R8758), DMEM media, FBS, RPMI1640, and antibiotic solutions were obtained from Gibco Laboratories. Metformin (# PHR1084), Fluo-3AM (#39294), 2-APB (#D9754), 5-BP (#914134), Z-gln-gly (#C6154), L -Glutamic acid γ-monohydroxamate (#G2253), tremeGENE 9 reagents such as siRNA and transfection reagents were procured from Sigma-Aldrich. FG-4592(Roxadustat) (#HY-13426) and TRPC6 antagonist BI-749327 (#HY-111925) were purchased from MedChemExpress, India. RNA purification reagents were purchased from Qiagen. cDNA Synthesis Kit (#6110A) from Takara and SYBR Green Master Mix reagents from Bio-Rad Laboratories. TRPC6 siRNA, ZEB2 siRNA were obtained from Santa Cruz Biotechnology. ChIP grade Protein-G agarose beads were purchased from CST. ProLong™ Diamond Antifade Mountant (P36961) purchased from Life Technologies. The primers used in the thesis were synthesized from Integrated DNA Technologies.

2.1.3.2 Animal handling and Hypoxia induction procedures:

The University of Hyderabad's Institutional Animal Ethics Committee accepted the animal study's experimental protocols. In this study, we employed Swiss albino male mice

that were 6 weeks old and weighed almost 30±5g. Water & food were provided to mice, ad libitum and mice were maintained at 37°C with 12/12 hrs light and dark cycles. These mice were randomly assigned to four groups (n=6): 1) control group, 2) FG4592 group, and 3) FG4592+Metformin group, 4) Metformin group. Experimental mice received a single i.p dose of FG4592 (5mg/kg/day) on each day for three months, whereas control mice have received an equal volume of PBS. The FG4592+Metformin treated group was received metformin (250mg/kg/day) per day through i.p, three hrs before FG4592 treatment, whereas the metformin group received metformin, only. After completing the experimental period, the mice's urine was collected to examine the proteinuria and estimate albumin and creatinine levels. After analyzing the urine, we have sacrificed the animals for further experiments. Under anesthesia, mice were perfused with saline. Organs were frozen immediately or fixed for histopathological investigation. Among both kidneys, one of the kidneys from each mouse is used to prepare the glomerular extract. Another is for staining and transmission electron microscopy imaging for morphological studies.

2.1.3.3 Silver staining:

Spot urine samples were collected from total mice and performed SDS-PAGE analysis and stained with silver nitrate as described earlier [50, 96]. One microliter of 1mg/ml of BSA is used as a standard, and 5 microliters of urine from Control, FG4592, and FG4592+Merformin group mice (n=6) were utilized for SDS-PAGE (10%) analysis and the silver staining was performed essentially as described earlier [50].

2.1.3.4 Human podocyte Cell Culture:

Immortalized human podocytes were gifted by Prof. Moin A Saleem (UoB, Bristol, UK) and were cultured as described earlier [50, 96]. Initially these podocytes were cultured at 33^{o}C and 5% CO_2 in RPMI-1640 and 10% FBS and these conditions known as growth

permissive conditions. To induce differentiation, these cells were shifted to 37ºC and 5% CO_2 and maintained for 14 days. Differentiated podocytes were used in all experimental procedures. 10mM stock of FG4592 was prepared in DMSO (treated with 10µM final concentration), and 1M stock of metformin was prepared in PBS (treated with 1mM final concentration).

Alternatively we also employed HEK293T cells for several experiments as these podocytes were difficult for transfection. HEK293T cells were cultured in DMEM media + 10% FBS. HEK293T cells were always cultured at 37°C with 5% CO_2. Experiments involved in treating both compounds, metformin was first treated for 3h and then treated with FG4592.

2.1.3.5 Immunoblotting:

An equal amount of total podocyte cell or glom lysate from control and experimental conditions was subjected to SDS-PAGE and performed immunoblotting essentially as described earlier [97]. After Immunoblotting, membranes were subjected to primary (1:1000) and secondary antibodies (1: 20000) and developed the blots using the Bio-Rad developing reagents. Image J software (NIH) was used to calculate band intensities.

2.1.3.6 Isolation of RNA and synthesis of cDNA:

RNA was isolated using Trizol reagent as manufacturer's protocol (Sigma) at room temperature (RT). Briefly, cells washed with PBS (ice-cold) and scrapped with PBS and subjected to brief centrifugation at 1000xg for 4 minutes. Trizol was added to the cell pellets and incubate for 5min at RT. 200 µl of chloroform was added and mixed vigorously. Samples were spun down at 12000 rpm for 15min at 4ºC and collected the upper transparent layer into a fresh tube. RNA was precipitated by adding half of the Trizol volume of propanol to the samples. Then, samples were spin down at 10000 rpm for 20min

at 4ºC to obtained RNA pellet. RNA pellets were washed with 75% ethanol and dried at 37ºC for 30min and resuspended in DEPC-treated water. Total RNA concentration was estimated by nanodrop, and one microgram of RNA was used as an input for cDNA synthesis. Similarly RNA was isolated from glomerular extracts of mice used in the study.

2.1.3.7 Quantitative Real-time PCR analysis:

Isolated RNA was used for cDNA synthesis using Takara kit and performed qRT-using the Kapa SYBR green master mix. The expression levels were normalized to either 18s rRNA or β-Actin, and the expression levels were quantified as a comparative (ΔΔCT) quantification method.

2.1.3.8 Immunofluorescence

Human podocytes were grown on coverslips up to 60% confluence, followed by treatment with FG4592 and metformin. After treatment, these podocytes were fixed with 4% paraformaldehyde, permeabilized with 0.1% Triton X-100 and blocked with 3% BSA in 1X PBS. Then, these podocytes were incubated with TGM2 antibody (1:100 dilution) and then Alexa labeled secondary antibody (1:200 dilution). Mounting was done by using the Prolong gold anti-fade DAPI. Fluorescence images were acquired with a trinocular microscope (Leica) with ×63 and ×100 magnification.

2.1.3.9 Histological Examination

4μM thickness paraffin sections were used and performed several stainings such as Masson's trichrome staining, PAS, and H&E staining. PAS and Masson trichrome staining show glomerular sclerosis and fibrosis, respectively. PAS and Masson trichrome staining show glomerular sclerosis and fibrosis, respectively. Renal cortex from control, FG4592, and FG4592, along with metformin-treated tissue samples, were fixed in 2.5% glutaraldehyde for 24 h, after washing with 1X PBS for four times, cortical tissues were fixed in 1% osmium tetroxide for 2 hours, and ultrathin sections (60 nm) were cut and

mounted on 200 mesh copper grids. These copper grids were stained on a Leica EM AC20 with 3% aqueous uranyl acetate and 3% lead citrate solution, and TEM analysis was performed as described earlier [50, 96].

2.1.3.10 Chromatin immunoprecipitation assay

Chromatin immunoprecipitation (ChIP) assay was performed as detailed earlier [50, 98]. Podocytes were treated with or without FG4592 for the stipulated duration. Following experimentation duration, chromatin was cross-linked using glutaraldehyde, and these crosslinks are revealed by glycine. The fragment size was 500bp and incubated with protein A beads/ ZEB2 antibody and pull down was purified and subjected to RT-qPCR using following primers. Forward 5′-GACCTAAGAGTCCACATCTG-3′ and Reverse 5′- CACAACTAGCCCAGGATAC-3′.

2.1.3.11 Fluo3-AM Staining for Ca^{2+} influx assay

As previously described, intracellular Ca2+ levels were measured in podocytes by staining calcium with Fluo-3AM dye [99]. Human podocytes were grown in 6-well plates ($1X10^6$ cells/well) and treated with or without 2-aminoethoxydiphenyl borate (2-APB) for 2 h. After cells were treated with FG4592 for 4h, the Fluo3-AM dye was added into each well at a concentration of 4uM and incubated for 0.5 hr. Cell lysates were prepared in calcium-free HBSS solution and spinned at 500 × g for 5 min and collected the supernatant. The supernatant was used to assess the fluorescence at λ485nm (excitation); λ538 (emission). The fluorescence maximum (Fmax) was achieved by adding 1% NP-40 to release maximum calcium bound dye from cells, and EGTA (0.5 M) was added to cell lysate to quench calcium and considered this as fluorescence minimum (Fmin). Intracellular free calcium was quantified by the formula ; $[Ca2+] = Fbasal - (Kd \times ((F - Fmin)/(Fmax - F)))$ where Kd for Fluo3-AM is 390 nM. The data expressed as relative calcium fold change.

2.1.3.12 TGM2 activity assay

We measured TGM2 activity in podocyte lysate as described earlier [100]. TGM2 activity assay utilizes the deamidation reaction of the transglutaminase enzyme with a donor and acceptor substrate resulting in the formation of a hydroxamate product. In this assay, CBZ-Gln-Gly, an amine donor, and hydroxylamine as an amine acceptor were used for the transglutamination reaction. In the presence of calcium and glutathione, TGM2 carries out a deamidation reaction and forms CBZ-glutaminyl-glycyl-hydroxamate, and can be measured at 525nm in a spectrophotometer. Briefly, the assay was conducted by incubating 100ug of total cell lysates containing no CaCl2 with 0.23mL incubation solution containing 31 mM CBZ-L-glutaminyl-glycine, 174 mM Tris, 4 mM CaCl2, 8.7 mM glutathione (GSH), and 87 mM hydroxylamine at final concentrations. After 10 min of incubation at 37^{O}C, 0.5 mL of 12% V/V TCA was added to precipitate the protein and substrate complexes for 5 min. After high-speed centrifugation, the final clear supernatant was measured at 525nm. The TGM2 activity is expressed in units/mg of protein catalyzes the formation of 1.0 µmole of hydroxamate per minute at pH 6.0 at 37°C.

2.1.3.13 Transfection of Plasmid DNA and siRNA

As discussed above, we employed HEK293T cells for transfection protocols as podocytes are resistant for transfection protocols. Before the day of transfection HEK293T, cells were seeded as monolayers at $1X10^5$ cells/well in 6-well plates and grown overnight at 37ºC in a 5% CO_2 incubator using DMEM media with 10% FBS. These cells were subjected to transfection with ZEB2 overexpression plasmid. Alternatively, HEK cells were transfected with ZEB2 siRNA and TRPC6 siRNA, respectively. The transfections were carried out using X-tremeGENE transfection reagents. Following 6h of transfection these HEK293T cells were treated with 10µM FG4592 for 24h. Cell lysates were analyzed by western blotting after transfection completion.

2.1.3.14 Statistical analysis

The data presented in this study as mean ± S.E. of at least three independent experiments. The data were analyzed using Prism software (GraphPad Software Inc.). One-way ANOVA was used to compare the groups. $p < 0.05$ was used to evaluate statistical significance.

2.1.4 Results

2.1.4.1 Expression of HIF1α and TGM2 in glomerular podocytes

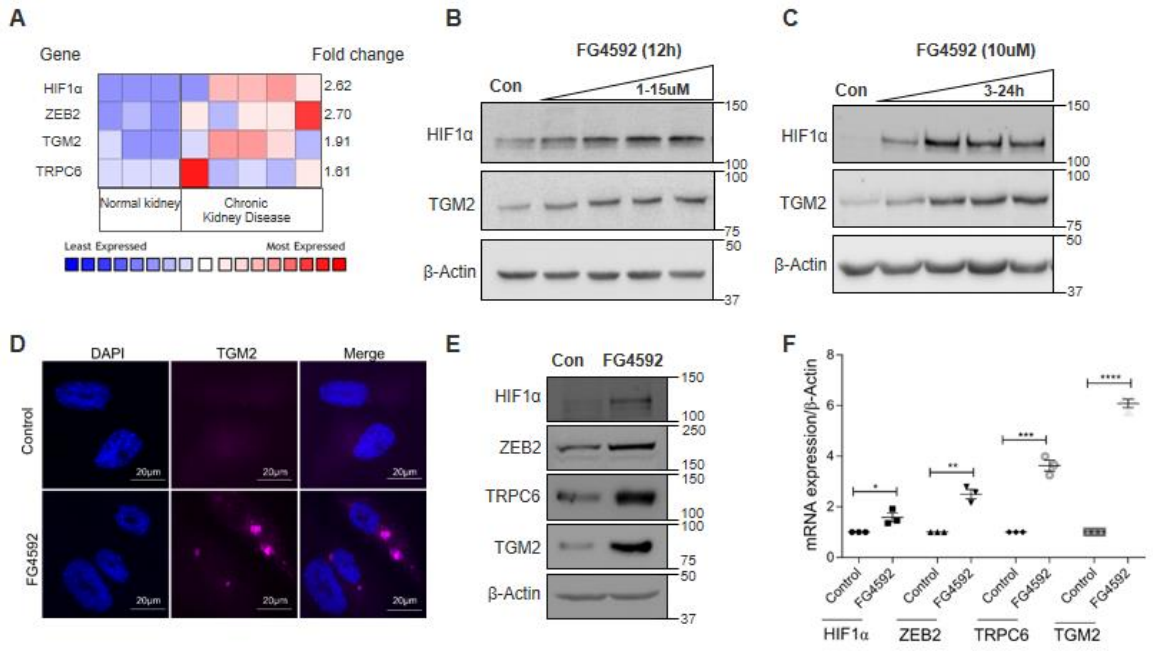

Figure 8. Stabilization of HIF1α by FG4592 stimulates TGM2 expression in podocytes. *HIF1α*, *ZEB2*, *TGM2,* and *TRPC6* expressions were analyzed between healthy volunteers (n=3) versus chronic kidney disease patients (n=5) in the validated set group of Nakagawa CKD kidney database in Nephroseq (www.nephroseq.org) (**A**). Immunoblotting analysis showing the expression of HIF1α, TGM2, and β-Actin in human glomerular podocytes treated with 1,5,10, and 15 μM of FG4592 for 12h (**B**) and with 10μM FG4592 for 3,6,12, and 24h (**C**). Immunofluorescence detection of TGM2 in control vs. FG4592 treated podocytes. Scale bar 20μm (**D**). Nephroseq data was validated in human podocytes exposed to 10μM of FG4592 for 24h by immunoblotting (**E**) and qRT-PCR. Error bars indicate mean ± SE; n=3. *, $p < 0.02$; **, $p < 0.001$; ***, $p < 0.0002$; ****, $p < 0.0001$ by student t-test (**F**).

We employed Nephroseq (https://www.nephroseq.org; UM, Ann Arbor) revealed co-expression of HIF1α, ZEB2 (Zinc finger E-box-binding homeobox 2), TRPC6 (Transient receptor potential channel 6), and TGM2 in Nakagawa CKD dataset (Fig.8A). To assess the specific role of HIF1α on TGM2 expression, we treated podocytes with FG4592 (known as Roxadustat, a prolyl hydroxylase inhibitor) in both dose (1-15uM; Fig.8B) and time-dependent manner (3-24h; Fig.8C) and found that stabilization of HIF1α by preventing hydroxylation resulted in elevated expression of TGM2. Intracellular localization of TGM2 in FG4592 treated podocytes was demonstrated by immunofluorescence (Fig.8D). Furthermore, we validated Nephroseq data and found that in addition to HIF1α, we noticed induction ZEB2, TRPC6, and TGM2 in podocytes treated with FG4592 (Fig.8E&F).

2.1.4.2 Elevated intracellular calcium levels associate with increased TGM2 activity

TGM2 is a calcium-dependent enzyme. Since we observed co-expression of TRPC6, a nonselective cation channel, and identified it as a component of store-operated calcium entry, we assessed calcium levels and TGM2 activity in FG4592 treated podocytes. We measured intracellular calcium using calcium-sensitive Fluo-3 AM dye and observed elevated calcium levels in podocytes treated with FG4592 (Fig.9A). Podocytes treated with 2-APB, an inhibitor of TRP channels, abrogated FG4592 induced calcium flux into podocytes (Fig.9A). Alternatively, FG4592 induced calcium influx was attenuated in human podocytes with where TRPC6 expression was abolished (Fig.9A). We next assessed TGM2 activity in podocytes in which TRPC6 expression was attenuated using siRNA, or TRPC6 activity was inhibited with 2-APB. Increased TGM2 activity was observed with FG4592 treatment, only partially reduced when podocytes were either co-treated with 2-APB or siTRPC6 (Fig.9B). We determined TRPC6 and TGM2 levels in podocytes treated with siTRPC6 by immunoblotting (Fig.9C&D). The data suggest reduced expression of TRPC6 by siRNA did not wholly abolish TGM2 expression in

FG4592 treated cells; this could explain the presence of residual TGM2 activity in cells with compromised TRPC6 expression. These observations suggest that, though increased intracellular calcium levels via TRPC6 elicits TGM2 activity, elevated TGM2 expression during hypoxia settings could further increase TGM2 activity.

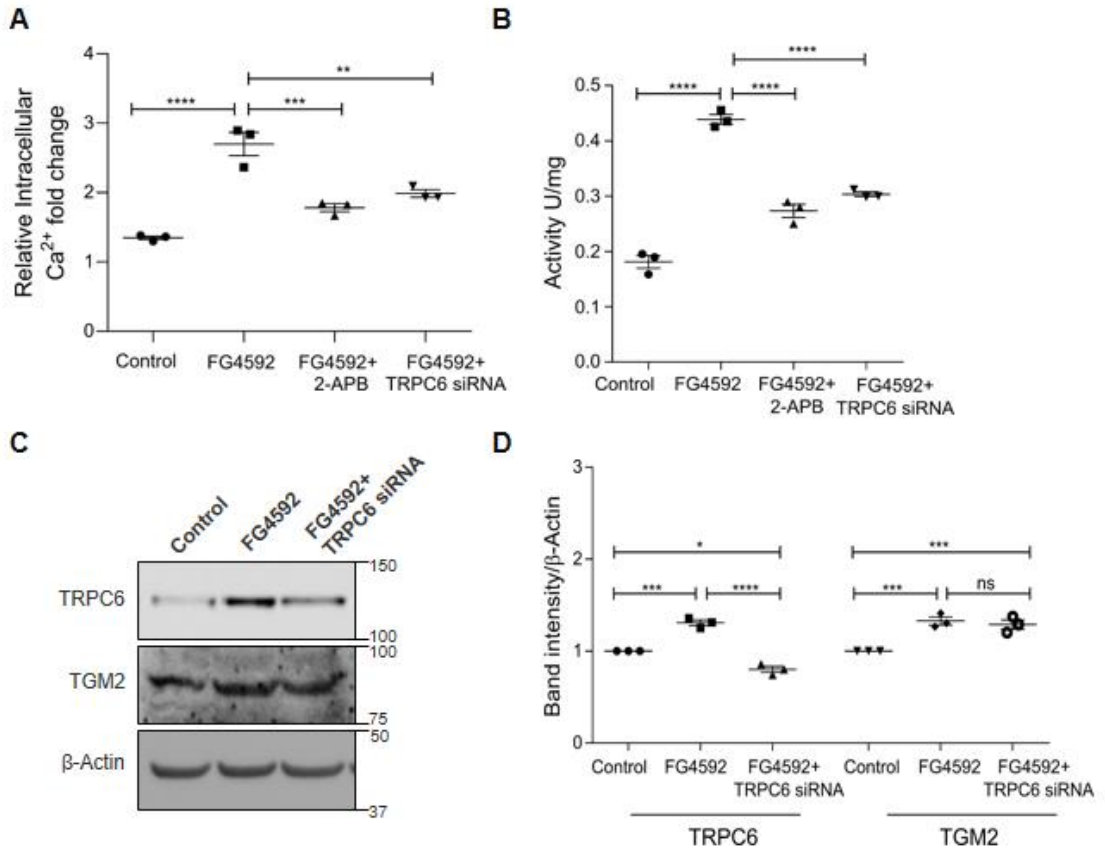

Figure 9. HIF1α promotes the TGM2 activity by inducing the calcium influx. Enhanced calcium influx was observed in FG4592 treated podocytes, whereas 2-APB and TRPC6 knockdown abrogated FG4592 induced calcium flux. Error bars indicate mean ± SE; n=3. **, $p < 0.001$; ***, $p < 0.0005$; ****, $p < 0.0001$ by one-way ANOVA after Tukey's multiple comparison test (**A**). TGM2 activity was measured in podocyte lysates from FG4592, 2-APB, and TRPC6 knockdown conditions. Error bars indicate mean ± SE; n=3. ****, $p < 0.0001$ by one-way ANOVA after Tukey's multiple comparison test (**B**). TRPC6 and TGM2 expression was assessed in podocytes treated with or without FG4592 and FG4592 along with the TRPC6 knockdown condition and quantified. Densitometric analysis of western blots was normalized to β-actin expression. Data presented as mean ± SE; n=3. *, $p < 0.01$; ***, $p < 0.0005$; ****, $p < 0.0001$ by one-way ANOVA after Tukey's multiple comparison test (**C&D**).

2.1.4.3 The essential role of ZEB2 in HIF1α induced TGM2 expression and activity

Since we observed TRPC6 knockdown does not eliminate TGM2 activity despite reduced intracellular calcium levels, we hypothesize that TGM2 expression is regulated differentially during hypoxia. It was shown earlier that ZEB2 is a bona fide target of HIF1α, and ZEB2 expression was induced in ischemic conditions [44]. We investigated the mechanistic insights since we observed co-expression of ZEB2 and TGM2 in the Nephroseq database and podocytes exposed to FG-4592 (Fig.8A&D) of this temporal association. We found three ZEB2 binding sites (E-box-binding region) upstream to the transcription start site of TGM2 in the range of -202 to -207; -238 to -243; -309 to -314 proximal promoter region of TGM2 (Fig.10A). Further, we performed a ChIP assay that revealed the binding of ZEB2 to the TGM2 promoter region (Fig.10B). N-cadherin promoter was utilized as a positive control as it possesses a putative ZEB2 binding site, and IgG acts as a negative control. Ectopically over-expressed ZEB2 resulted in elevated TRPC6 & TGM2 in HEK293T cells; in contrast, knockdown of ZEB2 abolished TRPC6 and TGM2 expression (Fig.10C). Interestingly, ZEB2 overexpression resulted in elevated intracellular calcium levels, while ZEB2 knockdown manifested in decreased intracellular calcium levels (Fig.10D), which is in tandem with TRPC6 expression. We next assessed TGM2 activity in podocytes in which ZEB2 ectopically overexpressed and ZEB2 silencing conditions. Increased TGM2 activity was observed with FG4592 treatment as well as in ZEB2 overexpressed conditions. Contrastingly, the ZEB2 silencing condition resulted in diminished TGM2 activity (Fig.E). The data suggests ZEB2 regulates TGM2 expression directly and its activity via inducing TRPC6 dependent calcium flux.

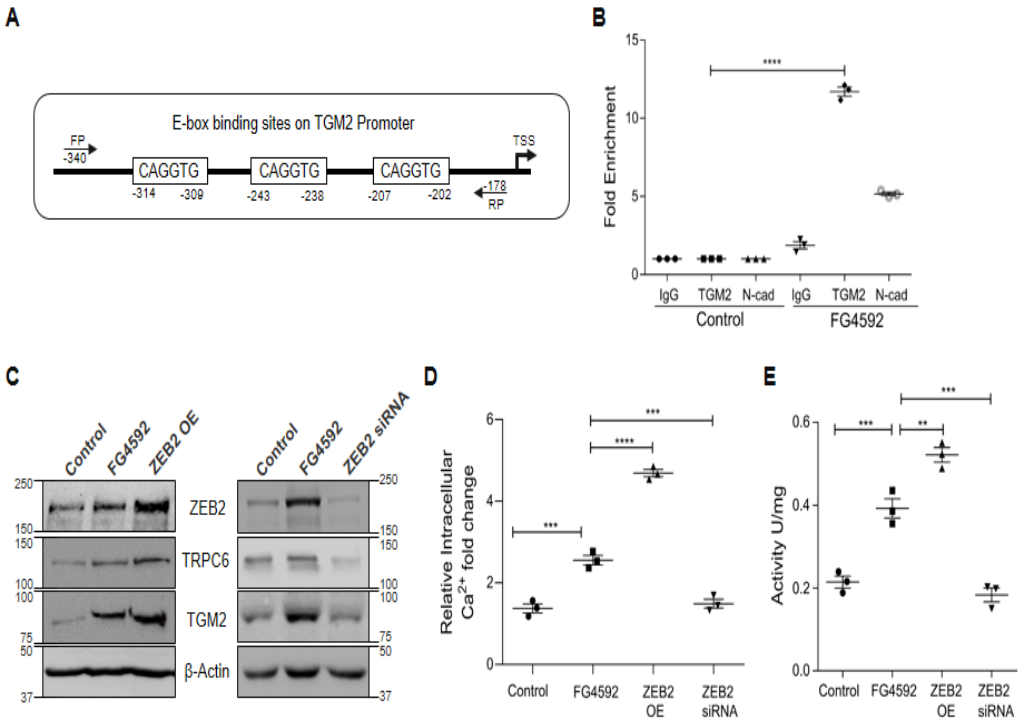

Figure 10. ZEB2 regulates the TGM2 expression directly and activity through TRPC6. The promoter region of TGM2 with ZEB2 binding E-box regions and region amplified following ChIP is indicated (**A**). ChIP analysis with chromatin fractions from podocytes exposed to FG4592. DNA from each of ChIP samples were PCR amplified for ZEB2 in the TGM2 promoter. E2-box in N-cadherin promoter serves as a positive control for ZEB2 interaction. Data presented as mean ± SE; n=3. ****, p< 0.0001 by one-way ANOVA after Tukey's multiple comparison test (**B**). Immunoblotting analysis showing protein levels of ZEB2, TRPC6, and TGM2 in HEK293T cells which are ectopically expressed ZEB2 and ZEB2 knockdown conditions (**C**). Enhanced calcium influx was observed in FG4592 treated podocytes along with ZEB2 overexpression and knockdown condition. Data presented as mean ± SE; n=3. ***, p < 0.0005; ****, p < 0.0001 by one-way ANOVA after Tukey's multiple comparison test (**D**). TGM2 activity was assessed in podocyte lysate treated with FG4592, ZEB2 overexpression, and ZEB2 knockdown conditions. Data presented as ± SE; n=3. **, p < 0.001; ***, p < 0.0005; by one-way ANOVA after Tukey's multiple comparison test (**E**).

2.1.4.4 Metformin suppresses HIF1α dependent TGM2 expression in vitro and in vivo

Since we observed stabilization of HIF1α resulted in accumulation of TGM2 and enhanced TGM2 activity, we assessed whether preventing HIF1α stabilization does affect

TGM2 expression and activity. In a recent study, Hart et al. demonstrated that metformin activates prolyl hydroxylases and ensures the degradation of HIF1α in mesothelial cells [101]; Metformin was shown to reverse hypoxia-induced migration by targeting the HIF1α/VEGF pathway in gall bladder cancer cells [102]. FG4592 induced stabilization of HIF1α and consequent accumulation of ZEB2 & TGM2 was attenuated in podocytes treated with metformin (Fig.11A&12A). Immunofluorescence data revealed the reduced TGM2 expression in podocytes that were treated with metformin (Fig.11B). Together, the data suggest that metformin prevents HIF1α accumulation and abolishes FG4592 induced activation of ZEB2/TRPC6/TGM2 axis in podocytes.

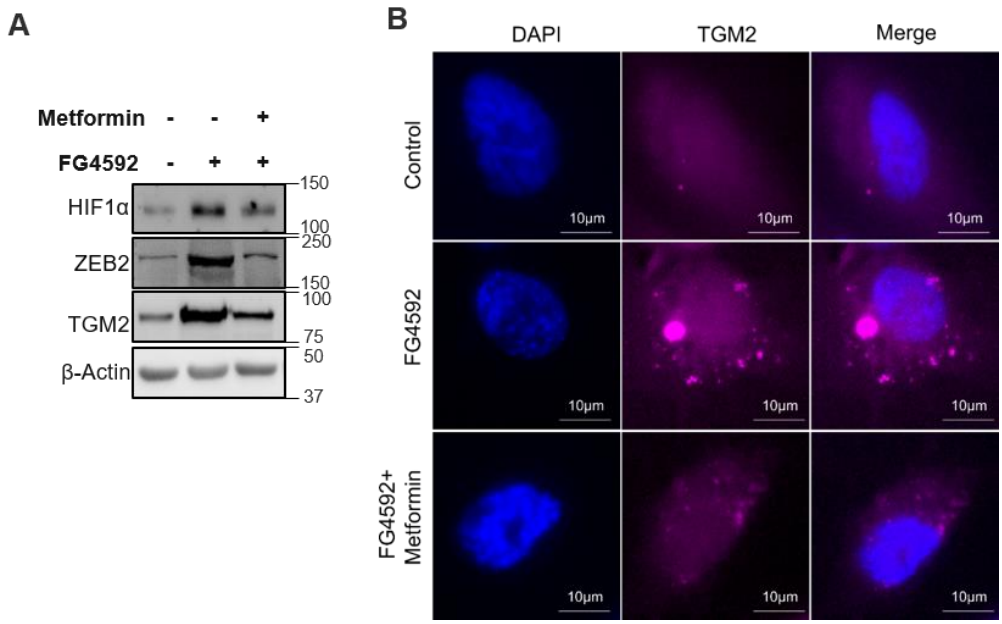

Figure 11. Metformin abrogates ZEB2 induced TGM2 expression. Metformin abolished FG4592 induced HIF1α, ZEB2, and TGM2 expression in human podocytes as analyzed by immunoblotting (**A**) and immunofluorescence. Scale bar 10μm (**B**).

2.1.4.5 Metfromin ameliorates hypoxia-induced renal fibrosis

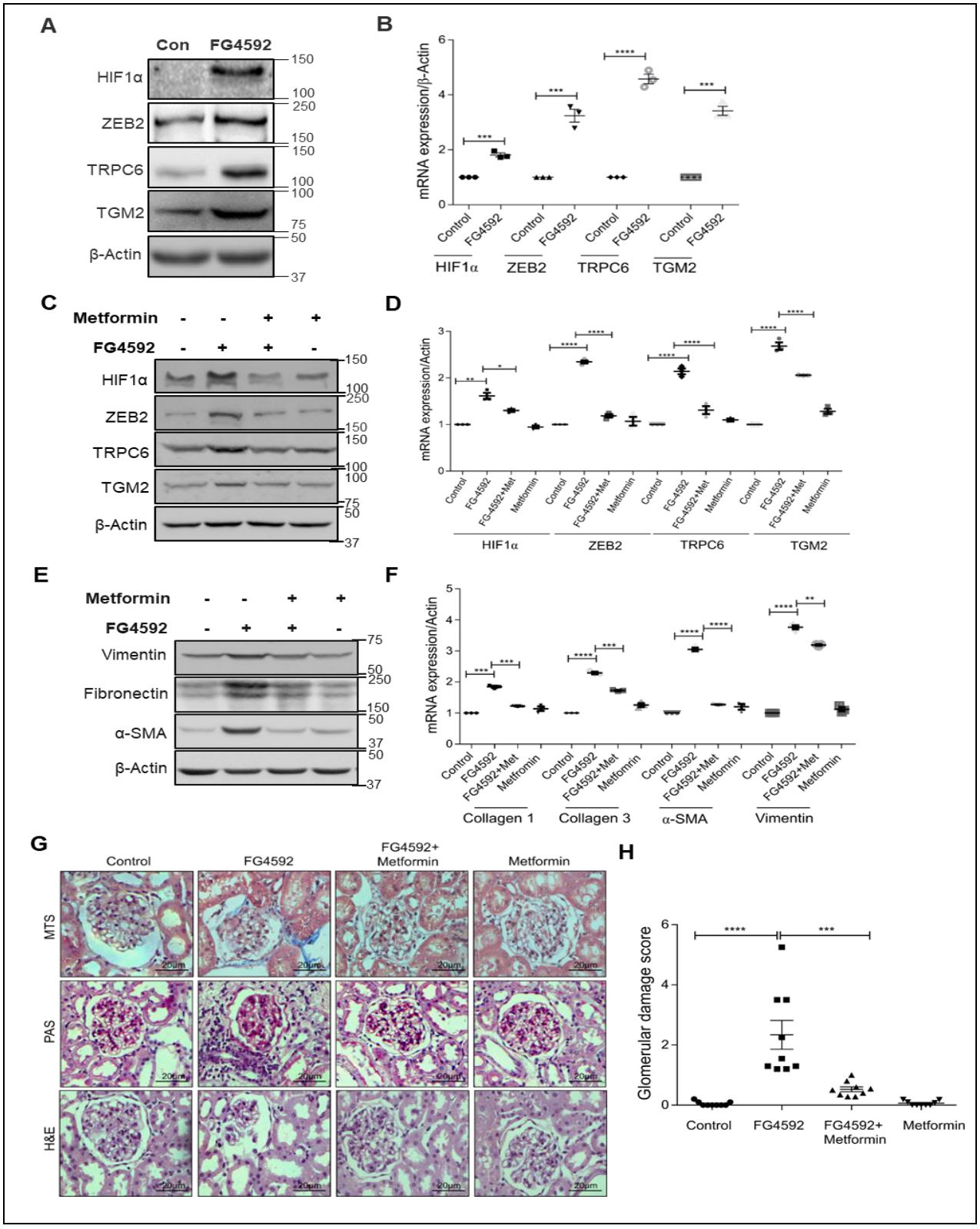

Figure 12. Metformin prevents hypoxia-induced glomerulosclerosis. Immunoblotting analysis of HIF1α, TRPC6, and TGM2 in glomerular lysate from mice administered with FG4592 in protein level (**A**) and qRT-PCR. Error bars indicate mean ± SE; n=3, ***, $p < 0.0002$; ****, $p < 0.0001$ by student t-test (**B**). Co-administration with or without metformin diminished the HIF1α, ZEB2, TRPC6, and TGM2 in immunoblotting (**C**) and qRT-PCR. Error bars indicate mean ± SE; n=3, *, $p < 0.02$; **, $p < 0.001$; ****, $p < 0.0001$ by student t-test (**D**). Immunoblotting analysis of fibrotic markers in glomerular lysate from mice administered with FG4592 and treated with or without metformin (**E**) qRT-PCR. Error bars indicate mean ± SE; n=3, **, $p < 0.001$; ***, $p < 0.0002$; ****, $p < 0.0001$ by student t-test (**F**). Masson's Trichrome Staining (MTS), PAS, and H&E staining of glomerular regions of mice were administered with FG4592 and treated with or without metformin. Scale bar 20μm (**G**). Glomerular damage analysis was performed as described in the methods section. Data presented as mean ± SE; n=9. ***, $p < 0.0005$; ****, $p < 0.0001$ by one-way ANOVA after Tukey's multiple comparison test (**H**).

Further, we investigated the effect of stabilization of HIF1α on TGM2 in vivo. Similar to in vitro studies, we observed elevated protein expression and mRNA expression of HIF1α, TRPC6, and TGM2 in glomerular lysate from mice administered with FG4592 (5mg/Kg b.w for 3 months) (Fig.12A&12B). In contrast, co-administration of metformin (250mg/Kg b.w for 3 months) prevented the activation of ZEB2/TRPC6/TGM2 axis in protein and mRNA level (Fig.12C&12D) and attenuated vimentin, fibronectin, and α-SMA expression both at protein and mRNA level (Fig.12E&12F). These three markers represent mesenchymal phenotype. We assessed the histological features by Masson's trichrome, H&E, and PAS staining in mice kidney sections (Fig.12G). Glomerular injury score analysis revealed metformin attenuated FG4592 induced fibrosis and altered histological features in glomerular and periglomerular regions as evidenced by glomerular injury score (Fig.12H).

2.1.4.6 Metformin prevents the hypoxia-induced proteinuria

Fibrosis causes the stiffening of the basement membrane that counteracts podocyte interactions with GBM leading to retraction of foot processes, called FPE. We performed transmission electron microscopy analysis in mice injected with FG4592 with or without metformin to study the foot process effacement. Our results show that metformin protected

the mice from FG4592 induced podocyte foot process effacement (Fig.13A). Metformin administration improved kidney function in FG4592 treated mice as evidenced by attenuation of proteinuria and UACR (Fig.13B&13C). These results suggest that metformin prevents renal fibrosis and foot process effacement in FG4592 treated mice, thus protecting them from proteinuria.

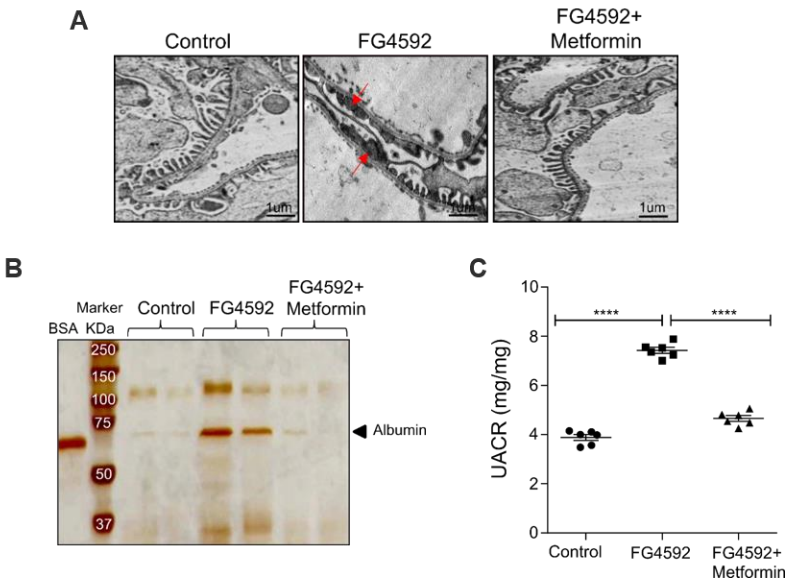

Figure 13. ***Metformin improves hypoxia-induced proteinuria.*** TEM images of podocytes from mice administered with FG4592 and treated with or without metformin. Arrow marks indicate the podocyte foot process effacement. Scale bar 1μm (**A**). Silver staining of urinary proteins from mice administered with FG4592 and metformin (**B**). Urine albumin to creatinine ratio (UACR) from mice administered with FG4592 and treated with or without metformin. Data presented as mean ± SE; n=6. ****, $p < 0.0001$ by one-way ANOVA after Tukey's multiple comparison test (**C**).

2.1.5 Discussion

Fibrosis represents a complex process where excessive deposition and cross-linking of ECM proteins occurs in concert with resistance of ECM components to breakdown by matrix matalloproteases. It has been known that TGM2 plays a vital role in cross-linking matrix proteins. Podocytes are instrumental for glomerular integrity and kidney function but localized conveniently to various noxious stimuli, including hypoxia,

hyperglycemia, and growth factors. HIF1α is implicated in several detrimental effects on podocytes [103]. In this particular chapter of my thesis, I investigated the mechanism of TGM2 regulation in clinical conditions that mimic hypoxia. Stabilization of HIF1α by FG4592 resulted in the accumulation of ZEB2 and its downstream target TRPC6. ZEB2 transcriptionally activates TGM2 expression, whereas, via TRPC6, it induces calcium influx, thus increase TGM2 activity. Blocking the TRPC6 action or suppressing its expression only partially attenuated FG4592 induced TGM2 activity, whereas suppression of ZEB2 expression significantly abolished TGM2 activity. This study demonstrates that stabilization of HIF1α stimulates both TGM2 expression and activity, whereas abrogation of HIF1α by metformin prevented HIF1α-regulated TGM2 and consequent glomerular injury.

HIF1α orchestrate the adaptive response of cells and tissue to the hypoxic environment by transcriptional activation of over a hundred of immediate and indirect downstream targets. The HIF1α targets regulate several vital biological processes such as erythropoiesis, angiogenesis, cell survival, cell metabolism, and epithelial-mesenchymal transition. ZEB2, an E-box binding homeobox 2 transcription factor, was reported to be a HIF target gene, and it induces TRPC6 expression in podocytes [44]. In this present study, we identified that ZEB2 regulates TGM2 expression directly. TGM2 promoter has E-box regions, and interaction of ZEB2 with TGM2 promoter is evidenced by chromatin immunoprecipitation, whereas ZEB2 knockdown significantly abolished TGM2 activity. On the other hand, inhibition of TRPC6 activity did not altogether abolish TGM2 activity. This study reports the complex and multi-level regulation of TGM2 by the ZEB2/TRPC6 axis in hypoxic conditions.

Besides catalyzing protein cross-linking and polyamination, TGM2 is an important mediator in gene regulation at various levels. In metastatic tumors detected in lymph

nodes and drug-resistant malignancies, increased TGM2 expression is linked to the development of EMT and stem cell-like features. [104, 105]. Interestingly, co-expression of ZEB2 and TGM2 was observed in the CKD dataset (Fig 8A) and metastatic cells [106]. TGM2 controls the transcription of genes by regulating the activity of NF-κB [107, 108]. Earlier reports showed that TGM2 regulates protein quantity by modifying and sequestrating proteins such as BAX-binding protein, caspase 3, and nucleophosmin [107, 109, 110]. A recent study showed that TGM2 regulates mRNA translation via enhancing mTORC1-mediated phosphorylation of 4EBP1 and cap-dependent translation in response to hypoxic stress [111]. The accumulating evidence suggests that targeting TGM2 could be a practical approach to combat EMT and metastasis or dealing with hypoxia-induced adverse manifestations. Therefore an adequate understanding of TGM2 regulation helps in dealing with clinical conditions in which TGM2 is implicated.

Earlier reports showed increased TGM2 activity and expression in hypoxic conditions. TGM2 expression was significantly up-regulated in chronic hypoxic rats and associated with right ventricular hypertrophy [112], whereas Hypoxia-induced pulmonary hypertension is linked to elevated TGM2 activity [113]. In contrast, studies showed that TGM2 is upstream of HIF1α and regulates the expression of HIF1α and its cellular targets. TGM2 interacts with p65/RelA, and this complex binds to the HIF1α promoter and induces its transcriptional activation [106]. Interestingly, inhibition of TGM2 abolished HIF1α expression and attenuated ZEB2 expression [106]. Though it is debatable whether TGM2 is upstream or downstream of HIF1α, ZEB2 appears to be a transcriptional target of HIF1α [44, 50, 96].

ZEB2, a SMAD-interacting transcription factor (known as SIP1) that plays a role in Mowat-Wilson syndrome, a congenital condition associated with kidney abnormalities [114]. Although studies reported that ZEB2 is necessary for normal nephron development

in mice [114], elevated ZEB2 levels were implicated in the EMT of podocytes suppressing E-cadherin expression [115]. ZEB2 induction is correlated with overexpression of transforming growth factor-beta-induced protein (TGFBI) in growth hormone (GH) treated podocytes and proteinuria in rats administered with GH [116]. TGFBI is an integral component of ECM, and it interacts with ECM proteins such as integrins and induces stabilization of microtubules [117]. Cerebral ischemia induces the HIF1α/ZEB2 axis in the glomerular podocytes and contributes to proteinuria [44]. The deleterious effects of the HIF1α/ZEB2 axis attributed to increased TRPC6 expression and resultant calcium influx into podocytes that resulted in aberrant activation of focal adhesion kinase [44]. Therapeutically inhibiting ZEB2 expression or TRPC6 expression is not a suggested option. Inhibition of ZEB2 expression suppresses TRPC6 expression and calcium conductance into a cell. It was recently reported that decreased TRPC6 expression in TRPC6 −/− podocytes resulted in calpain mislocalization and considerable down-regulation of calpain activity, which resulted in the modified cytoskeleton of podocyte and its motility & adhesion [118]. Therefore, blocking HIF1α accumulation or targeting TGM2 active site inhibitors appears to be therapeutic options.

2.2 Screening inhibitors for TGM2

2.2.1 Abstract:

Transglutaminases are enzymes that catalyze the alteration of proteins after they have been translated. TGM2 is the widely studied member of this family, which catalyzes the cross-linking via N-ε-(γ-glutamyl) lysine bonds between the side chains of peptide-bound Glutamine and Lysine residues. Accumulation of TGM2 client proteins is found in renal fibrosis. In this study, we screened chemical compounds structurally similar to the GTP, an allosteric inhibitor of TGM2. We screened 1985 compounds from the PubChem database against TGM2 GTP binding pocket. There are three compounds we selectively identified that show the highest binding energy and obeyed Lipinski's properties. These compounds did not show any structural deviations in the peptide backbone of TGM2. Further, our analysis suggests that they show better interaction in comparison to the GTP molecule, thereby may act as potential therapeutic inhibitors against TGM2 and abate the progression of renal fibrosis.

2.2.2 Introduction:

TGM2, widely known as tissue transglutaminase, is an extracellular calcium-dependent transferase enzyme (EC: 2.3.2.13) that catalyzes the formation of N-ε-(γ-glutamyl) lysine cross-links between peptide side chains [76]. Transglutaminase (TGM2) ensures the formation of a stable dipeptide bond that results in proteolytic-resistant, intra and intermolecular cross-links of client proteins. TGM2 client proteins include several ECM proteins, including collagen, laminin, osteopontin, fibronectin, and fibrinogen. TGM2 dependent cross-linking of ECM proteins enables the stabilization of collagen fibrils, reduced proteolysis, thus results in the accumulation of ECM proteins. The potential character of TGM2 is to catalyze the iso-peptide bond formation and cross-linking of ECM components and thus renal fibrosis [76, 82]. Since the accumulating evidence suggests that the catalytic activity of TGM2 is implicated in the pathobiology of an array of diseases, inhibition of the TGM2 activity could be a therapeutic strategy to combat an array of diseases in which elevated activity of TGM2 is implicated.

Accumulating evidence suggests that the catalytic activity of TGM2 is implicated in the pathobiology of an array of diseases and inhibition of the TGM2 activity could be a potential strategy to combat these diseases. Several research investigators developed irreversible inhibitors such as Halomethyl carbonyls, 3-Halo-4, 5-dihydroisoxazole, and competitive inhibitors resembling acyl-donor substrate were tested in both cell culture (*in vitro)* and *in vivo* models. Nevertheless, a clinically validated TGM2 inhibitor is yet to be obtained for human use.

This study screened reversible inhibitors for TGM2 using a GTP-Structure similarity-based approach and a combination of both protein-ligand docking and molecular dynamic techniques. Based on the structural similarities with GTP, we screened 1985 compounds that best fit the GTP binding pocket of TGM2. Structure prediction and

molecular dynamics simulations identified three potent chemical compounds with the highest binding affinity and most minor or no degree of alterations in the protein backbone after binding. These three inhibitors could be further validated to treat pathologies in which TGM2 is implicated.

2.2.3 Methods:

2.2.3.1 Ligand retrieval, validation, and preparation:

To find potential TGM2 inhibitors, we screened and considered compounds similar to the GTP to mimic the TGM2 enzyme inactivation by GTP (open conformation). We manually searched for the ligands in the PubChem database using the following parameters (Table.3). The shortlisted compounds from the PubChem were further screened as follows. The SMILES information of the shortlisted compounds was submitted to the SwissADME server (http://www.swissadme.ch/). This server analyzed the compounds physicochemical, lipophilicity, water-solubility, pharmacokinetics, drug-likeness, and medicinal chemistry features.

Table.3: Parameters used in PubChem for searching ligands for inhibiting TGM2.

Parameters	Values
Molecular Weight	200-1100 g/mol
Rotatable Bond Count	0-20
Heavy Atom Count	10-60
H-bond Donor Count	2-15
H-bond Acceptor Count	5-34
Polar Area	100-600 Å
Complexity	300-2200
XLogP	(-10) -1

Further, we verified whether the ligands followed Lipinski's rules at pH 7.0 using the supercomputing facility (http://www.scfbio-iitd.res.in/software/drugdesign/lipinski.jsp)

located at for Bioinformatics and Computational Biology server of IIT Delhi Toxicology screening was also done using the vNN-ADMET Webserver (https://vnnadmet.bhsai.org/) to assess the ligand's mutagenicity, cytotoxicity, microsomal stability, hepatotoxicity, cardiotoxicity, and drug-drug interactions. Only the compounds that passed these criteria were selected for docking with the TGM2 enzyme.

2.2.3.2 Molecular docking of compounds with TGM2:

We next docked the GTP and the shortlisted compounds that could bind to the GTP pocket of the TGM2 enzyme. The 3D coordinates of the TGM2 enzyme were gathered from the RCSB protein data bank (PDB ID: 2Q3Z). The GTP and compounds were prepped by detecting their torsion roots, and polar hydrogen atoms were added using the Avogadro software. GTP and the shortlisted compounds were docked to the GTPase pocket of the TGM2, which consist of the residues Arg476, Arg478, Arg580, Phe174, Met483, and Val479.

2.2.3.3 Molecular Dynamic (MD) simulations:

Only the compounds that showed a better docking score than the GTP were considered for MD simulation using Gromacs 5.1.4. We performed MD simulations for the empty TGM2 and TGM2 docked with the GTP as controls. The topology of the ligands was generated in the CGenFF (https://cgenff.umaryland.edu/), and the CHARMM36 force field was used to run the simulations. The complexes were centered in 5.073 x 5.831 x 16.180 nm boxes and solvated with the Simple point charge (SPCE) water system. 18 Na+ ions neutralized the systems' total net charge. The steepest descent minimization method was then used to do energy minimization and system equilibration. At a steady temperature and pressure of 300K and 1atm, the system was equilibrated for 100 picoseconds. We next used the long-range electrostatics were then treated with particle-mesh Ewald approach, following which the simulations were carried out for 100 nanoseconds. After the

MD simulations, we analyzed the protein-ligand interactions using the PDBsum server and LigPlot. Also, we plotted the root mean square deviation (RMSD), root mean square fluctuation (RMSF), and the radius of gyration (Rg) of the complex using XMGrace.

2.2.3.4 Molecular docking of selected compounds with other enzymes GTP binding pocket:

We further docked the GTP and the shortlisted compounds with the GTP pocket of other proteins such as Ras homolog gene family, member A (Rho A), Ras associated with diabetes (Rad), Small GTP binding protein Gem. The 3D coordinates of the selected proteins were gathered from the RCSB protein data bank (PDB ID: 1A2B, 2DPX, 2CJW respectively). By measuring the torsion roots of the GTP and selected compounds, polar hydrogen atoms were added. The selected proteins GTPase pockets were docked with GTP and the shortlisted compounds. The docking was performed in auto dock vina.

2.2.4 Results:

2.2.4.1 Screening and validation of potential TGM2 inhibitors:

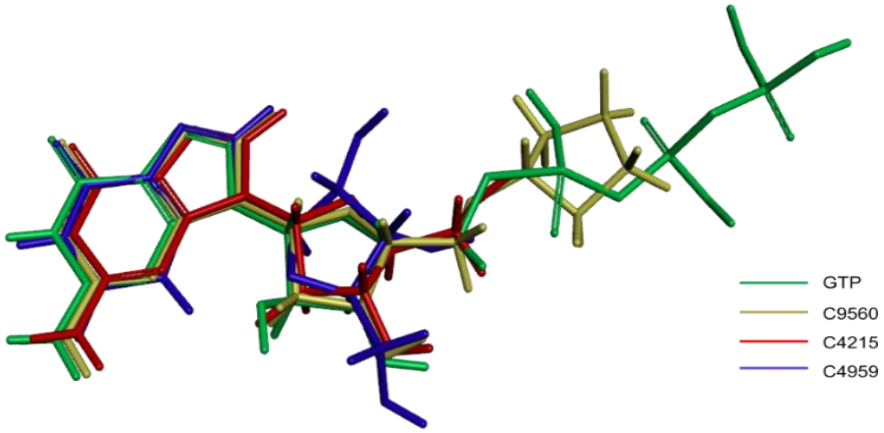

Figure 14: ***Superimposition of all molecules.*** The superimposition of three finalized molecules along with GTP. GTP (Green), C9560 (Yellow), C4215 (Red), C4959 (Blue). The structures of ligands were obtained from the PubChem database.

Based on the structural similarity and parameters submitted to the PubChem, a total of

1985 compounds that were either similar or had a sub-structure of GTP were identified. Further, screening these compounds by the SwissADME server shortlisted 150 compounds with a bioavailability score of ≥0.55 and obeyed Lipinski's rules were selected. Toxicology analysis of these 150 compounds revealed 86 compounds safe and suitable for further studies. We next docked these 86 compounds and the GTP molecule into the GTPase site of the TGM2 and predicted their docking scores. A docking score of -7.0 Kcal/mol for GTP was chosen as the threshold to shortlist the compounds further. Four novel compounds with PubChem IDs, namely, CID_137274215, CID_136349560, CID_135600340, and CID_64959 (from here on referred to as C4215, C9560, C0340, and C4959) that showed the structural similarity with the GTP (Fig.14, Table.4) showed docking scores ≥ GTP.

Table 4: Accession numbers, IUPAC names, and structures of TGM2 inhibitors.

PubChem ID	IUPAC Name	Structure	Abbreviated Name
CID_135398633	[[(2*R*,3*S*,4*R*,5*R*)-5-(2-amino-6-oxo-1*H*-purin-9-yl)-3,4-dihydroxyoxolan-2-yl] methoxy-hydroxyphosphoryl] phosphono hydrogen phosphate	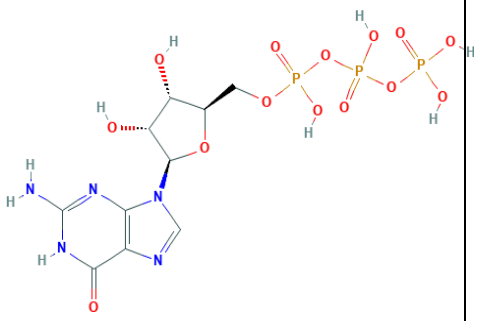	GTP
CID_136349560	2-amino-9-[(2*R*,4*S*,5*R*)-5-(cyclopentyloxymethyl)-4-hydroxyoxolan-2-yl]-1*H*-purin-6-one	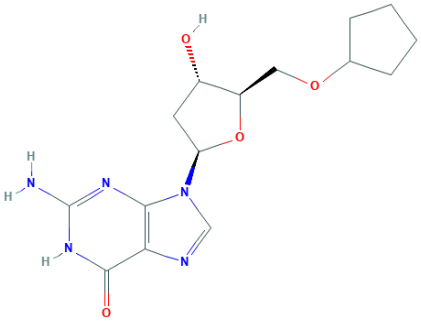	C9560

CID_137274215	2-amino-9-[(3*R*,4*S*,5*S*)-3-fluoro-4-hydroxy-5-(hydroxymethyl) oxolan-2-yl]-1*H*-purin-6-one	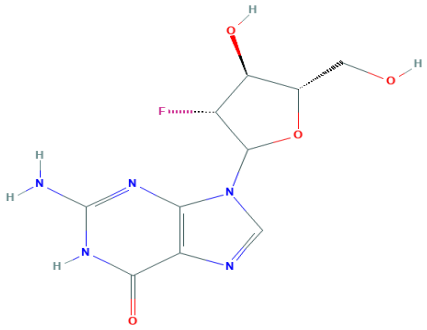	C4215
CID_64959	9-[(2*R*,3*R*,4*S*,5*R*)-3,4-dihydroxy-5-(hydroxymethyl) oxolan-2-yl]-3*H*-purine-2,6-dione	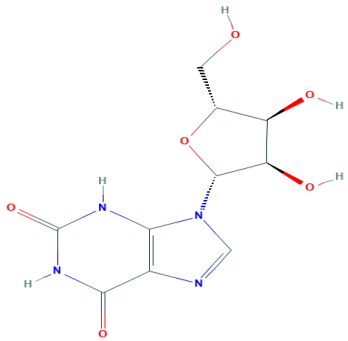	C4959

2.2.4.2 Docked complexes of TGM2 with ligands:

We performed Molecular Docking for the TGM2 protein with selected ligands. We have docked to the GTP binding pocket of the TGM2 Protein. All ligands are docked to the GTP binding pocket. We took the GTP molecule as a positive control. The docking score of TGM2+GTP is -7.0. We have selected the ligands more than -7.0. The docked complexes are shown in (Fig.15). These Compounds are delivering the best fit to the GTP binding pocket of TGM2.

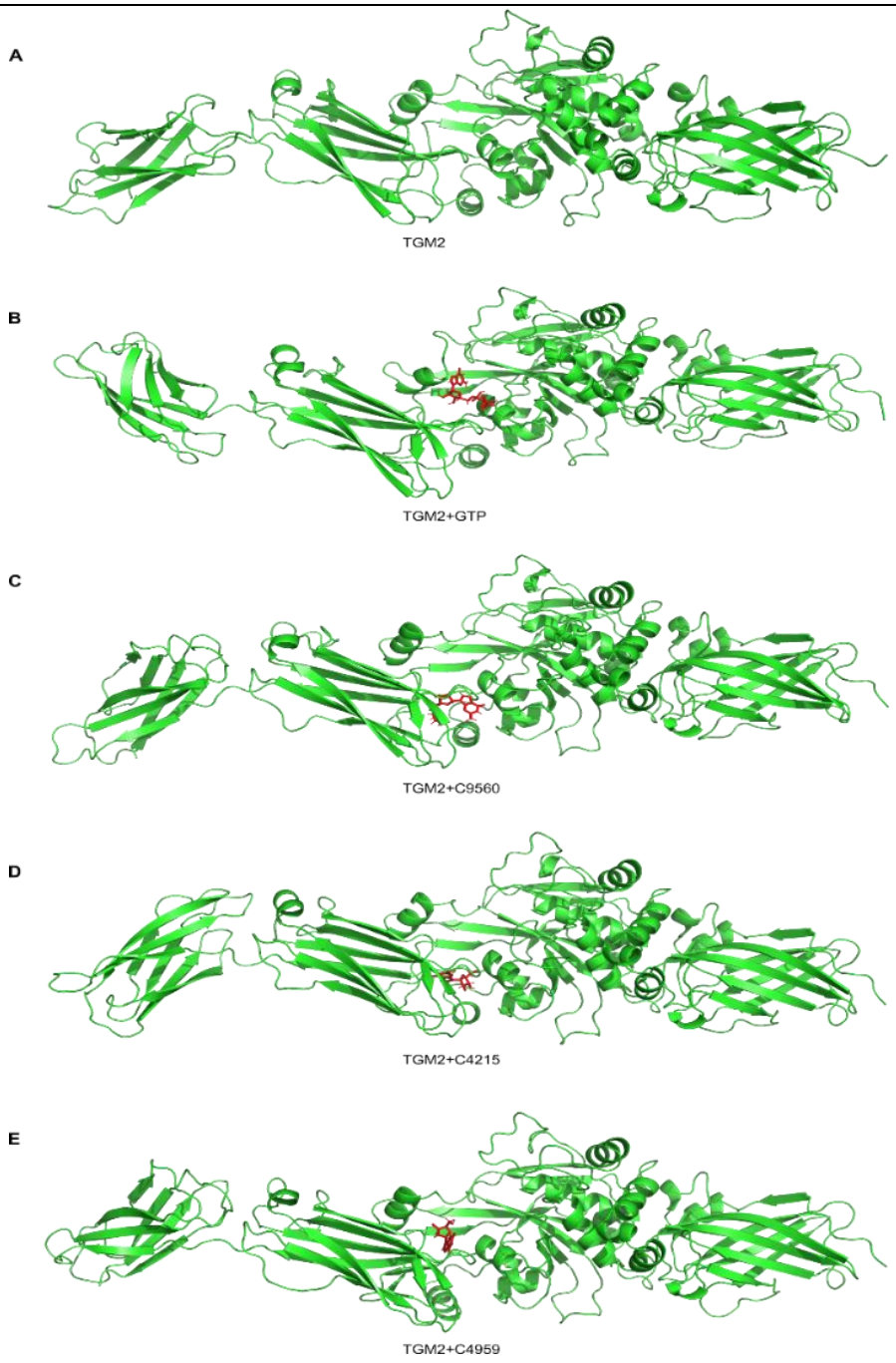

Figure 15: ***TGM2 and ligand docked complexes.*** TGM2 Protein in green colour and ligands in red colour. **A.** Empty TGM2 Protein **B.** TGM2+GTP docked structure **C.** TGM2+C9560 docked structure **D.** TGM2+C4215docked structure **E.** TGM2+C4959 docked structure.

2.2.4.3 Molecuar Simulatons:

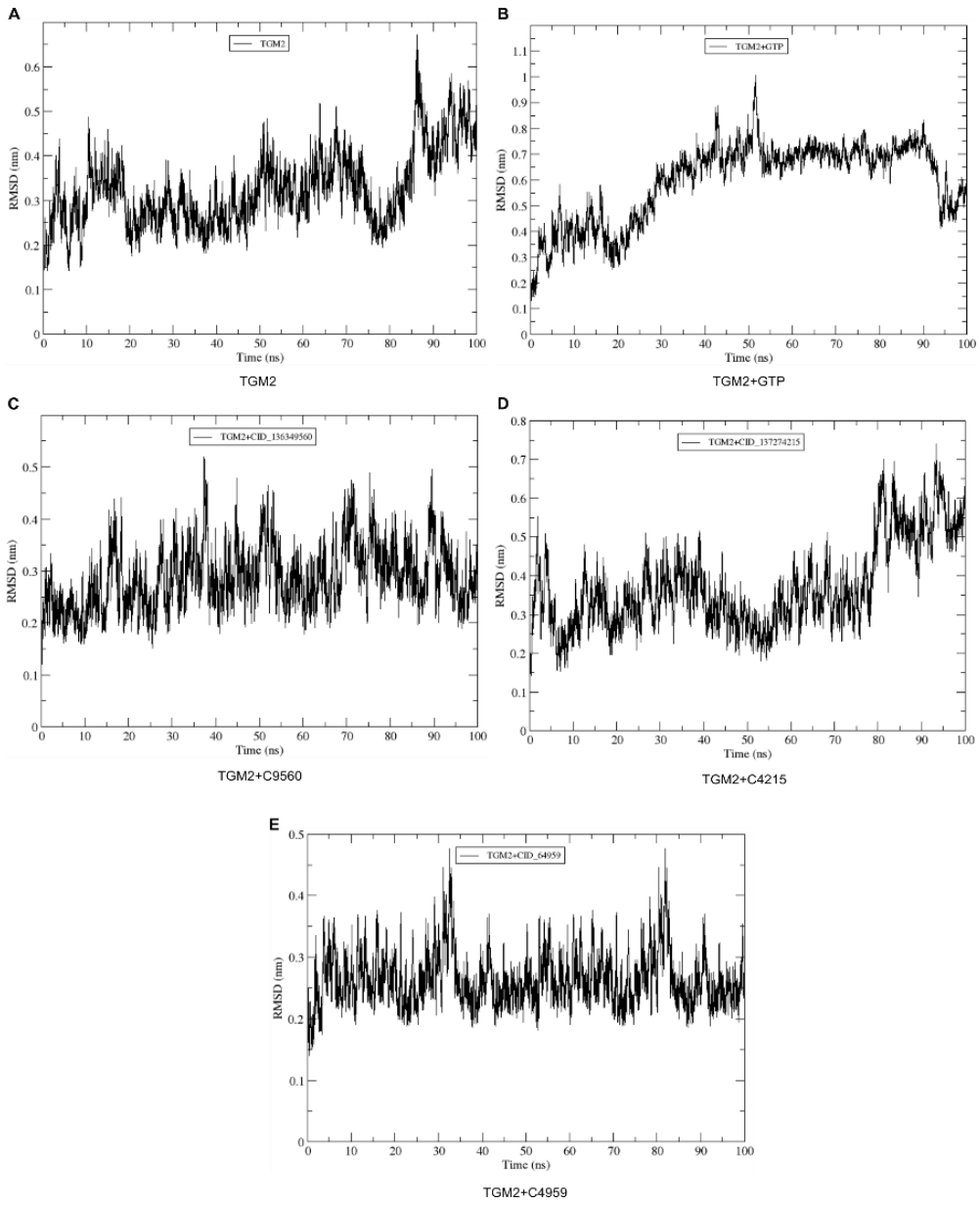

Figure 16: **RMSD graphs of TGM2 and ligand complexes after simulation.** *The simulation run time was 100ns.* ***A.*** *Empty TGM2 Protein* ***B.*** *TGM2+GTP RMSD graph* ***C.*** *TGM2+C9560 RMSD graph* ***D.*** *TGM2+C4215 RMSD graph* ***E.*** *TGM2+C4959 RMSD graph.*

We performed MD simulations for the TGM2 protein, and TGM2 docked with GTP, C4215, C9560, and C4959 complexes. To understand the stability of the complexes, we plotted RMSD vs. time plots for TGM2 and TGM2-ligand complexes (Fig.16A-E). The RMSD of TGM2 fluctuated between 0.2-0.4 nm (Fig.16A), whereas the TGM2-GTP complex showed an initial RMSD fluctuation between 0.2-0.4nm until 30ns, after which it increased to 0.6-0.8nm until ~92ns followed by a drop to 0.4-0.5ns until 100ns (Fig.16B). In the case of the TGM2-C4215 complex, the RMSD fluctuation until 80ns was between 0.25-0.4nm, after which it increased to 0.5-0.7nm (Fig.16C). Unlike the TGM2 bound to GTP or C4215, the RMSD fluctuation of the TGM2-9560 and TGM2-C4959 complexes was constant between 0.2-0.3nm throughout the simulation (Fig.16D & E). These results suggest that the complexes TGM2-9560 and TGM2-4959 showed the least RMSD compared to the enzyme and other complexes suggesting that C9560 and C4959 may form stable complexes with TGM2.

Similarly, we plotted RMSF per residue plots for TGM2 and TGM2 complexes. The data suggest that RMSF for residues 1-600 was constant at ~0.15nm (Fig.17A-E), nevertheless significant jumps in RMSF for the residues 601-686 with peaks reaching up to 0.6-0.7nm for TGM2 and TGM2 complexes (Fig.17A-E). This data may suggest that the C-terminal segment (residues 601-686) was flexible throughout the simulation.

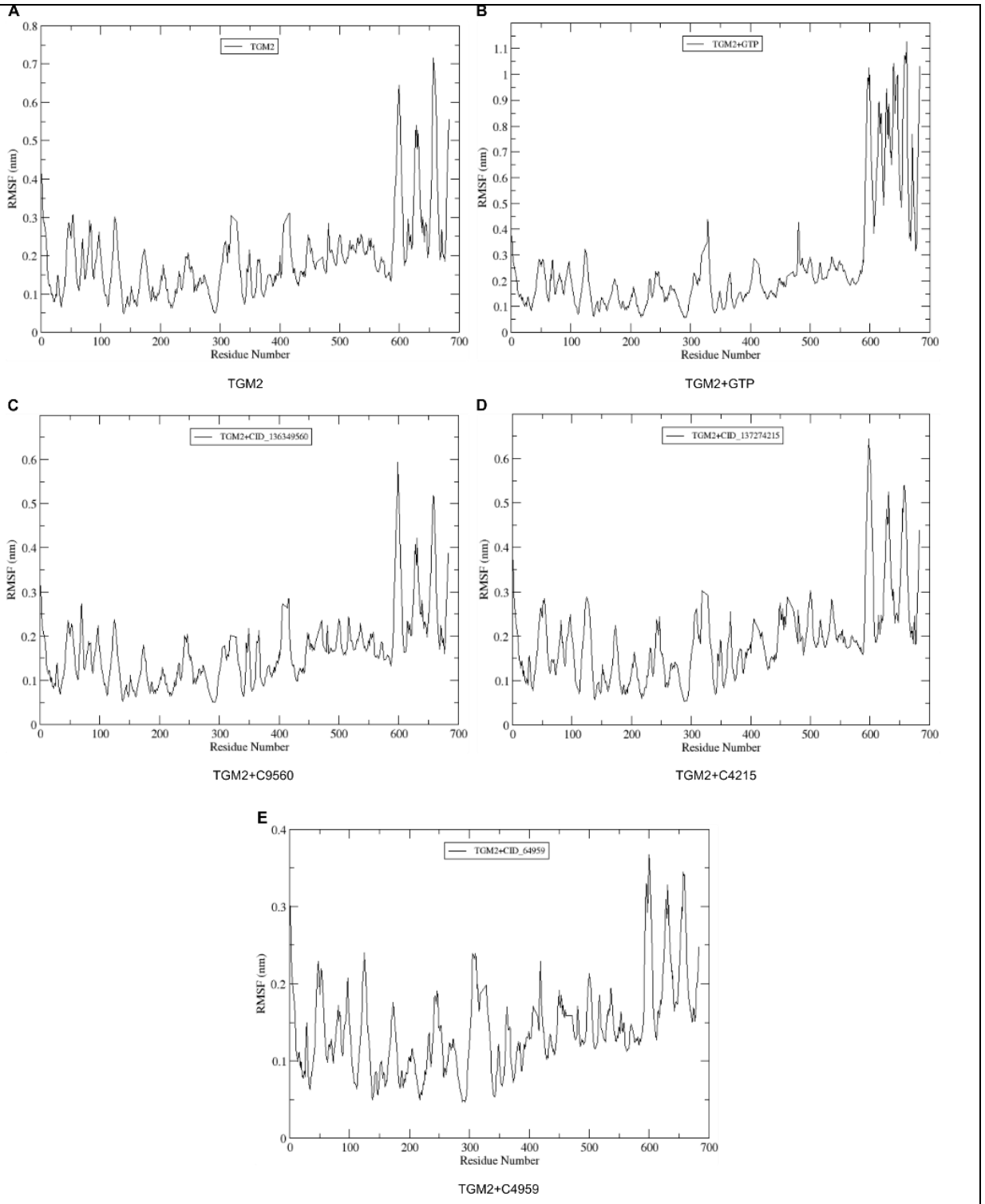

Figure 17: ***RMSF graphs of TGM2 and ligand complexes after simulation.*** The simulation run time was 100ns. **A.** Empty TGM2 Protein **B.** TGM2+GTP RMSF graph **C.** TGM2+C9560 RMSF graph **D.** TGM2+C4215 RMSF graph **E.** TGM2+C4959 RMSF graph.

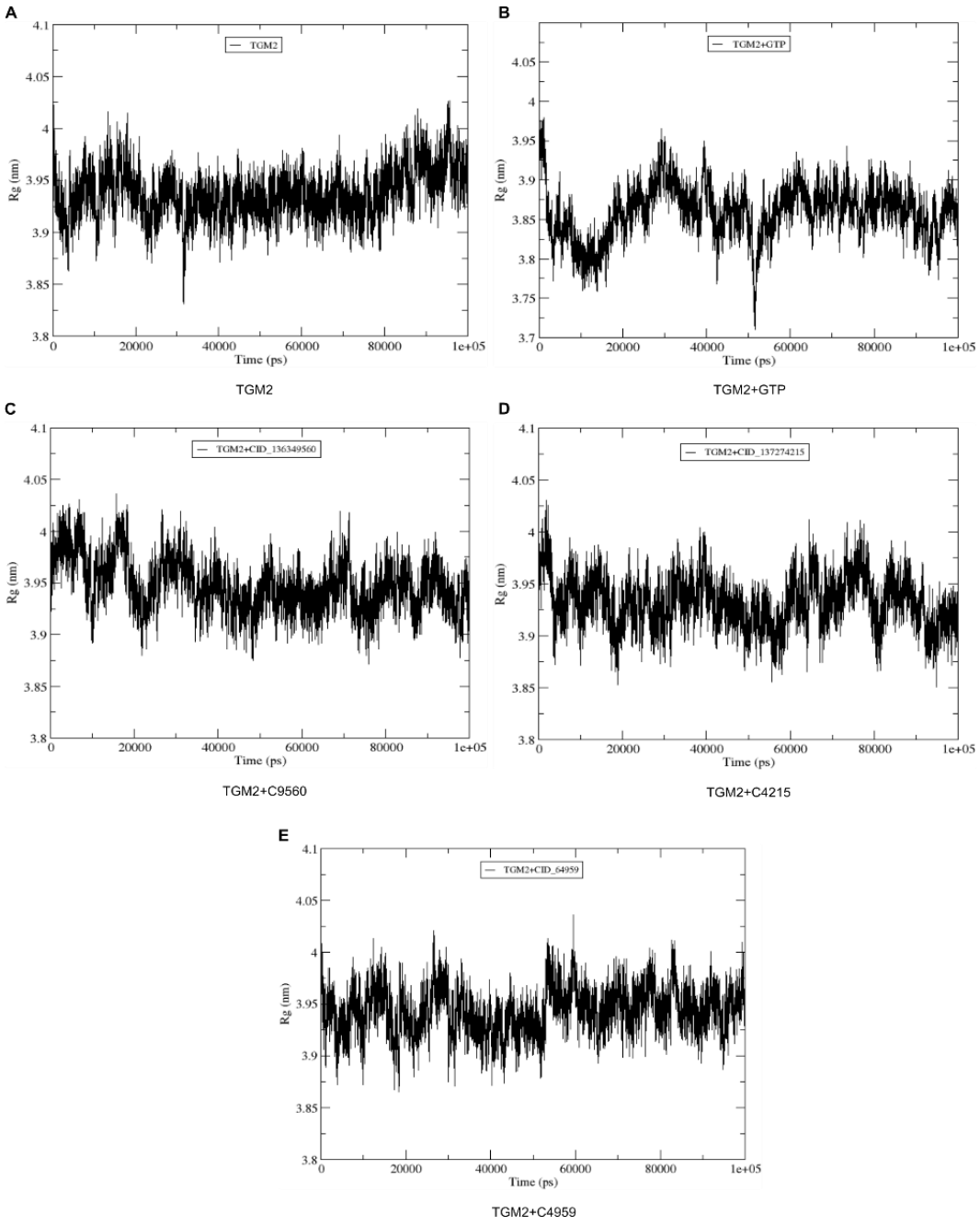

Figure 18: ***Rg graphs of TGM2 and ligand complexes after simulation.*** The simulation run time was 100ns. **A.** Empty TGM2 Protein **B.** TGM2+GTP Rg graph **C.** TGM2+C9560 Rg graph **D.** TGM2+C4215 Rg graph **E.** TGM2+C4959 Rg graph.

Similarly, we plotted Rg vs. time plots for TGM2 and TGM2 complexes (Fig.18A-E). The Rg measures the compactness of the protein/protein-complexes as the simulation progress, thus giving an insight into the protein/protein-complexes stability.

Our results showed that the Rg plots of TGM2 and TGM2 complexes did not show any significant fluctuations. However, a slight dip in Rg was detected in the case of the TGM2-GTP complex for the initial 20ns, after which the Rg was similar to the rest of the TGM2 and TGM2 complexes. Collectively our data suggest that the novel compounds formed stable complexes with the TGM2 enzyme.

2.2.4.4 C9560 formed a stable complex with TGM2:

Our results suggest that the unique compounds show greater affinity towards TGM2 in comparison to GTP (Table.3). Further, we observed that C9560 showed the highest affinity (-8.0 Kcal/mol) towards TGM2, followed by C4215 and C4959. Interestingly, the interacting residues of TGM2 with the novel compounds and the GTP differed significantly (Table.5). Apart from the predicted hydrogen bonds, several non-bonded contacts are present between the TGM2 and the novel compounds. The hydrogen bonds with TGM2 protein with ligands showed in the lig plots (Fig 19).

Table 5: The hydrogen-bonded residues involved in the interactions with the ligands after MD simulations.

Compound Name	Before Simulation	After Simulation				
	Docking score with TGM2 (Kcal/mol)	Docking score with TGM2 (Kcal/mol)	Compound atom name	TGM2 residues	TGM2 atom name	Distance (Å)
GTP	-7.0	-7.0	O6 O2B O3G	Arg317 Phe392 Asn573	NE O OD1	2.82 1.27 1.95
C4215	-7.3	-7.2	O3 O3 O1	Phe394 Ile572 Leu576	O O N	2.99 3.33 2.96
C9560	-7.0	-8.0	O4	Ser574	O	2.43
C4959	-7.0	-7.0	N3	Ser574	N	2.01

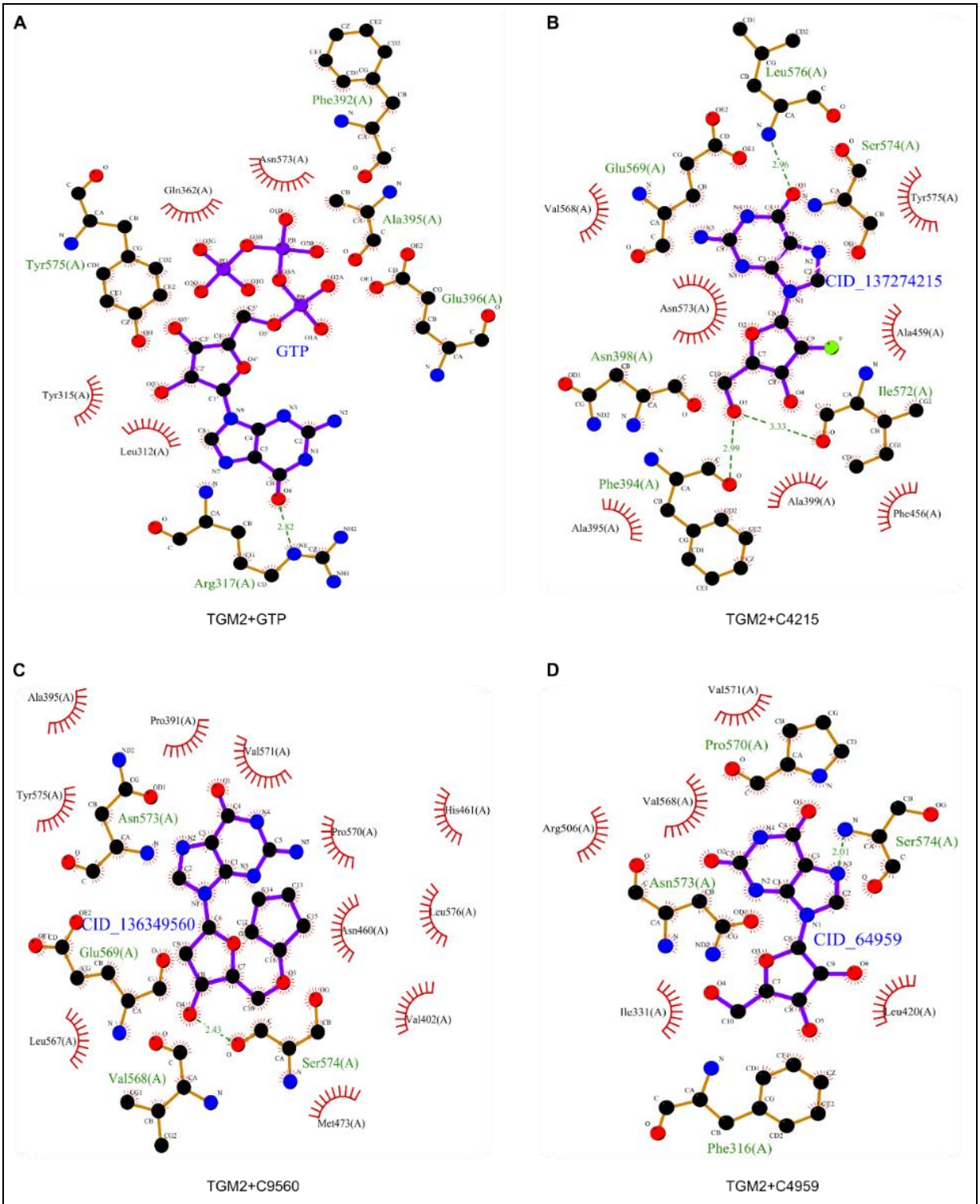

Figure 19: ***Ligplots of TGM2 with ligand complexes after simulation.*** Ligplot shows the interacting binding residues between TGM2 Protein and ligands. Green colour labeled residues are involved in the hydrogen bonding with TGM2 Protein. Green colour dotted lines show the distance between TGM2 Protein and ligands. **A.** TGM2+GTP Ligplot **B.** TGM2+C9560 Ligplot **C.** TGM2+C4215 Ligplot **D.** TGM2+C4959 Ligplot.

2.2.4.4 Verification of interaction of ligands with GTP binding pocket of related enzymes:

In order to verify the specificity and selectivity of the inhibitors i.e ligands what we screened for TGM2, we performed the docking with few related enzymes (RhoA, RAD, and GEM) that possess GTP binding pockets. Our analysis suggest that the shortlisted three compounds have predominantly greater affinity towards TGM2 in comparison to other selected proteins as revealed by docking score (Table.6). The only exception we noticed was with C9560, which showed the slightly higher affinity (-8.1 Kcal/mol) for RAD over TGM2. The results suggest that screened and shortlisted compounds (C4215, C9560, and C4959) are giving the best fit to the GTP binding pocket of TGM2 when compare to other small GTP binding proteins.

Table 6: Docking scores of selected ligands with selected proteins.

Compound Name	Docking score (Kcal/mol)			
	TGM2	Rho A	RAD	GEM
GTP	-7.0	-8.9	-12.7	-9.1
C4215	-7.3	-5.9	-6.7	-5.8
C9560	-7.0	-6.4	-8.1	-7.0
C4959	-7.0	-5.2	-6.2	6.1

2.2.5 Discussion:

The activity of TGM2 is believed to be up-regulated and is implicated in the pathology of number of diseases. Although the involvement TGM2 in the pathology of cancer, celiac neurological diseases, and renal diseases was investigated, the precise molecular mechanism by which TGM2 contributes to these diseases has not been elucidated. Based on its involvement researchers suggested that TGM2 could be a potential therapeutic

target against an array of ailments including fibrosis during chronic kidney disease [82]. Researchers strongly believe that inhibition of TGM2 offers significant protection against hypoxia-induced maladaptive tissue repair. Therefore, my study is aimed to investigate the possible inhibitors against TGM2. In this study, we screened large number of inhibitors for TGM2 to the GTP binding pocket and short-listed only three compounds as TGM2 inhibitors. These compounds were filtered according to the GTP structure using the docking and simulation studies.

Although the precise in vivo function of TGM2 remains enigmatic, multiple pieces of evidence revealed its role in various etiologies, and inhibition of TGM2 was suggested as a target from a therapeutic perspective. Among different modes of inhibition, reversible inhibitors may help to block the enzyme under physiological conditions. Therefore, in this study, we used strategies to screen many inhibitors and found that the compounds were identical to GTP, screened them using the pharmacophore approach, and validated their interaction and inhibition with the allosteric site of TGM2. We also verified that the three compounds that were short-listed showed enhanced interaction than GTP.

Both GTP and GDP are cofactors for TGM2, acting as allosteric and reversible inhibitors [90]. The GTP analogs such as GMP-PCP and GTPγS reversibly inhibit TGM2 [90]. Since reversible inhibition of enzymes shown to be effective [76], we used a similar strategy to screen the inhibitors that could interact with TGM2 identical to that of GTP. Interacting capacity analysis revealed that the short-listed molecules (C9560, C4215, and C4959) that resemble GTP and differ from each other in side-chain modification could interact with TGM2 more effectively than GTP. Like GTP, we predict that our selected molecules can work as allosteric and reversible inhibitors for the TGM2 enzyme. We have performed a simulation for 100ns with the selected ligands with the TGM2 enzyme to strengthen our data. Our simulation data revealed that the selected compounds are more

stable than GTP in RMSD, RMSF, and Rg.

Like GTP, our selected molecules also will show the allosteric and reversible inhibition towards TGM2. TGM2 reversible inhibitors prevent the TGM2 activity by halting the substrate availability to the catalytic site without modifying the enzyme covalently. These inhibitors have delayed binding kinetics, implying that they bind to TG2 independently of GTP, possibly via competing for the same binding site. Recently, the Case group has identified the unique set of reversible & allosteric inhibitors with the backbone of thieno [2,3-*d*]pyrimidin-4-one acyl hydrazide. They have shown that their molecules are extensively binding with the GTP binding pocket of TGM2 based on their kinetic analysis [119, 120].

Further studies are required to validate whether these GTP analogs could inhibit TGM2 and prevent TGM2 associated pathologies. Owing to COVID-19 restrictions we were unable to perform synthesis of these compounds and pre-clinical research in mice. However, few days ago our lab initiated in vivo studies to investigate the therapeutic potential of identified inhibitors. It is noteworthy that the shortlisted compounds are less likely interacting with other enzymes that possess GTP binding pocket.

3. Summary

The kidneys are vital organs that regulate water and electrolyte balance, thereby maintains the body's homeostasis. These organs continuously exposed to body fluids and are thus vulnerable to various noxious stimuli and physiological factors that curb human physiology. It is largely considered that kidney fibrosis is the final common insult that leads to end-stage kidney failure. Kidney is composed of several cell types including podocytes, endothelial cells, mesangial cells, and tubular cells. Due to the high cell-type heterogeneity, targeting kidney fibrosis becomes exceptionally challenging. Glomerular podocytes are one of the essential cell types that play a crucial role in regulating glomerular filtration and also help to maintain integrity of the glomerulus by contributing to the glomerular basement membrane and endothelial cells. Interestingly, podocytes express both epithelial and mesenchymal cell markers at healthy states, however these cells switch to a mesenchymal state when they injured, particularly during nephropathic conditions that present with proteinuria. Increasing evidence indicates that podocytes are at extreme risk during chronic kidney injury. Noxious milieu during chronic kidney disease (CKD) conditions including hypoxia drives podocyte injury and resulting in varying degrees of proteinuria.

The continuous glomerular filtration and tubular reabsorption are energy required processes. Since energy requirement by renal cells is very high, the demand for synthesizing sufficient ATPs is very high. Therefore, the demand for ATP is met by oxidative phosphorylation. Together, the high demand for oxygen supply for the glomerular and tubular function renders kidneys to hypoxic exposure, making kidneys more susceptible to damage in diseases particularly involved with glomerular dysfunction. Hypoxia has been characterized to play a crucial role in driving fibrosis, which is implicated in the end-stage kidney dysfunction. Besides fibrosis, hypoxia is implicated in the several cellular phenomenon such as epithelial-mesenchymal transition and angiogenesis, which

in turn influence the renal health and implicate in the kidney disease, which are mediated by HIF1α. A Blood oxygen level-dependent magnetic resonance imaging study demonstrated that low tissue oxygenation is an independent predictor of lowering kidney function [121]. A recent method using a lifetime phosphorescence imaging probe BTPDM1 (benzothienylpyridine dimethylamino) identified hypoxic in chronic kidney disease condition [122].

Relative renal hypoxia exists in adolescents with type1 diabetes mellitus associated with albuminuria, suggesting hypoxia is a common factor in chronic kidney disease and diabetic kidney disease [123]. Hypoxia is also related to cardiovascular disease and patients with chronic vascular complications develop chronic kidney disease over time. Indeed, hypoxia has been associated with stroke-induced proteinuria. However, the mechanism of stroke-induced proteinuria was initially being solved in our lab. We showed that HIF1α transcriptionally induces ZEB2 in podocytes of rats with middle cerebral artery occlusion (MCAO), an ischemic model widely used to generate stroke in rodents [50]. ZEB2 suppresses the expression of E-cadherin and ZO-1 tight junction proteins and induces mesenchymal markers, including N-cadherin and Vimentin, in one arm. On the other hand, ZEB2 expression induces TRPC6, a calcium channel activity that facilitates hyper calcium influx into podocytes resulted in podocyte structural changes leading to proteinuria in MCAO [44]. Therefore, the HIF signaling is considered a dominant factor in cerebrovascular, cardiovascular, diabetic kidney disease conditions.

The classic view that targeting hypoxia could prevent fibrosis progression has been the paradigm for several decades. In recent advance investigations suggesting that the consequences of targeting hypoxia signaling using HIF1α inhibition to treat kidney disease showed varying outcomes in murine models. In contrast, inhibition of HIF1 hydroxylases is also protective against experimental fibrosis [124]. Moreover, oral administration of Roxadustat, a HIF1 activator, is being used in clinical trials for anemic patients with CKD

[125]. Therefore, the elements directly involved in the progression of ECM stabilization or kidney fibrosis would be helpful for patients with acute or chronic renal failure. TGM2 is an extracellular matrix cross-linking and stabilizing enzyme whose expression was highly correlated with kidney fibrosis. TGM2, along with several ECM proteins, have been characterized to be the direct targets of HIF1α. Moreover, several ECM proteins are the direct substrates for TGM2 transamination activity, suggesting that HIF1α partially relies on TGM2 expression and activity in the process of kidney fibrosis.

Given the importance of HIF signaling in kidney injury, our lab longed an interest in understating the hypoxia-driven mechanisms in podocyte injury. Although our prior publications showed elevated calcium levels in hypoxia, the main focus was completely different. In this thesis, I demonstrated that ZEB2 transcriptionally induces TGM2 expression and increases activity by TRPC6 expression and mediated intracellular calcium pools in podocytes exposed to hypoxic conditions. The Abrogation of HIF1α improved renal function by suppressing TGM2 expression and activity in ZEB2/TRPC6 manner.

The salient findings of my study are:

- Stabilization of HIF1α by FG4592 stimulates TGM2 expression in glomerular podocytes *in vitro* and *in vivo*. There is a temporal association between the expression of HIF1α and TGM2.
- ZEB2, a downstream target of HIF1α, also regulates TGM2 expression (via interacting with promoter) and activity via elevated intracellular calcium levels via TRPC6.
- Knocking down of ZEB2 expression could able to prevent TGM2 activity only partially. This could be due to HIF1α induced TRPC6 expression, which sequesters Calcium, a co-factor for TGM2.

- Inhibition of HIF1α by metformin abolished ZEB2 and, in turn, TGM2 expression.
- Metformin prevents hypoxia-induced glomerulosclerosis and improved kidney function.
- Out of the 1985 compounds screened, we short-listed only three compounds that showed the highest binding energy with TGM2 by obeying Lipinski's physicochemical properties, ADME, and Toxicology profile.
- Our study also revealed that the seleted ligands are more specific for TGM2 only, and are not interacting with GTP binding pockets of other enzymes of matrix such as RhoA, and GEM.
- In summary, our study revealed that stabilization of HIF1α stimulates TGM2 expression & activity, whereas abrogation of HIF1α protected from TGM2 induced renal manifestations and improved kidney function. Targeting TM2 with the selected ligands could be the potential strategy to combat hypoxia-induced renal complications. Further studies will work with the selected compounds targeting TGM2 and test their potency on renal fibrosis mouse models.

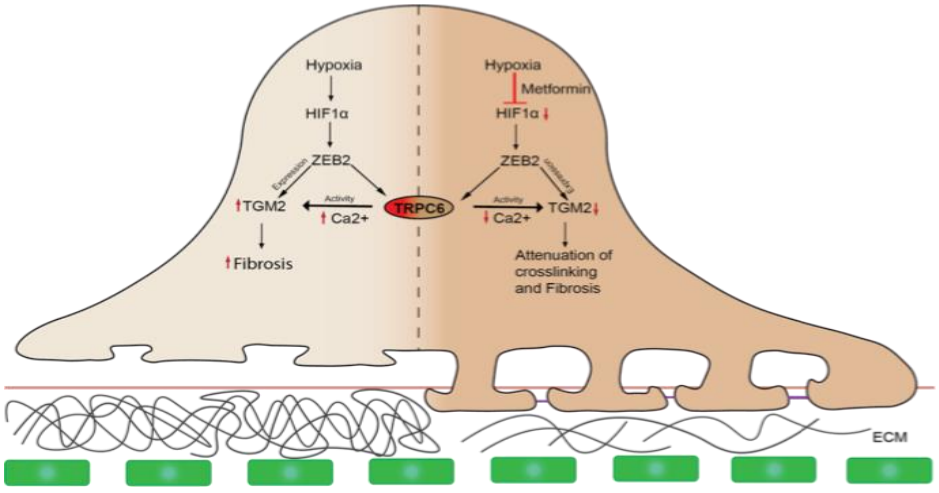

Figure 20: A schematic representation of metformin action on FG4592 induced podocyte pathogenesis.

The findings detailed in this thesis was publishing as follows:

1. **Kolligundla LP et al.,** ZEB2/TRPC6 axis transduce HIF1α dependent regulation of Transglutaminase 2 in glomerular podocytes. (Manuscript submitted to JCP and ID. JCP-21-1091).

2. **Kolligunlda LP et al.,** Identification of potent reversible inhibitors for Transglutaminase 2. (Manuscript communicated to International Journal of Simulation Modelling).

Related manuscripts:

3. Singh AK*, **Kolligundla LP*** et al., Detrimental effects of hypoxia on glomerular podocytes. JPB, 2021; doi -10.1007/s13105-021-00788 (*Equal contribution).

4. Nakuluri K, Nishad R, Mukhi D, Kumar S, Nakka P.V, **Kolligundla LP** et al., Cerebral ischemia induces TRPC6 via HIF1alpha/ZEB2 axis in the glomerular podocytes and contributes to proteinuria. Sci Rep, 2019; 9(1): p.17897.

5. Mulukala SK, Nishad R, **Kolligundla LP** et al., *In silico* Structural characterization of podocin and assessment of nephrotic syndrome-associated podocin mutants. IUBMB Life, 2016; 68(7):578-88.

4. References

1. Kumar, P.A., et al., *Carboxymethyl lysine induces EMT in podocytes through transcription factor ZEB2: Implications for podocyte depletion and proteinuria in diabetes mellitus.* Arch Biochem Biophys, 2016. **590**: p. 10-19.
2. Ogobuiro I, T.F., *Treasure Island (FL).* StatPearls, 2021.
3. Basi, S., et al., *Microalbuminuria in type 2 diabetes and hypertension: a marker, treatment target, or innocent bystander?* Diabetes Care, 2008. **31 Suppl 2**: p. S194-201.
4. Kumar, P.A., P.S. Chitra, and G.B. Reddy, *Metabolic syndrome and associated chronic kidney diseases: nutritional interventions.* Rev Endocr Metab Disord, 2013. **14**(3): p. 273-86.
5. Weissgerber, T.L. and L.M. Mudd, *Preeclampsia and diabetes.* Curr Diab Rep, 2015. **15**(3): p. 9.
6. Anil Kumar, P., et al., *Molecular and cellular events mediating glomerular podocyte dysfunction and depletion in diabetes mellitus.* Front Endocrinol (Lausanne), 2014. **5**: p. 151.
7. Zhou, D., et al., *Sonic hedgehog connects podocyte injury to mesangial activation and glomerulosclerosis.* JCI Insight, 2019. **4**(22).
8. Bryer, J.S. and K. Susztak, *Screening Drugs for Kidney Disease: Targeting the Podocyte.* Cell Chem Biol, 2018. **25**(2): p. 126-127.
9. Pollak, M.R., et al., *The glomerulus: the sphere of influence.* Clin J Am Soc Nephrol, 2014. **9**(8): p. 1461-9.
10. Lin, J.S. and K. Susztak, *Podocytes: the Weakest Link in Diabetic Kidney Disease?* Curr Diab Rep, 2016. **16**(5): p. 45.
11. *Communication Skills: Definitions and Examples.* Shine learning.com.
12. Pavenstadt, H., W. Kriz, and M. Kretzler, *Cell biology of the glomerular podocyte.* Physiol Rev, 2003. **83**(1): p. 253-307.
13. Miner, J.H., *The glomerular basement membrane.* Exp Cell Res, 2012. **318**(9): p. 973-8.
14. Reiser, J. and M.M. Altintas, *Podocytes.* F1000Res, 2016. **5**.
15. Fukasawa, H., et al., *Slit diaphragms contain tight junction proteins.* J Am Soc Nephrol, 2009. **20**(7): p. 1491-503.
16. Kriz, W., *Glomerular diseases: podocyte hypertrophy mismatch and glomerular disease.* Nat Rev Nephrol, 2012. **8**(11): p. 618-9.
17. Nagata, M., *Podocyte injury and its consequences.* Kidney Int, 2016. **89**(6): p. 1221-30.
18. Timpl, R. and J.C. Brown, *Supramolecular assembly of basement membranes.* Bioessays, 1996. **18**(2): p. 123-32.
19. Liu, Y., *Renal fibrosis: new insights into the pathogenesis and therapeutics.* Kidney Int, 2006. **69**(2): p. 213-7.
20. Eddy, A.A., *Molecular basis of renal fibrosis.* Pediatr Nephrol, 2000. **15**(3-4): p. 290-301.
21. Stocum, D.L., *Handbook of Stem Cells (Second Edition).* 2013.
22. Yoshida, M. and S. Honma, *Regeneration of injured renal tubules.* J Pharmacol Sci, 2014. **124**(2): p. 117-22.
23. Sugimoto, H., et al., *Renal fibrosis and glomerulosclerosis in a new mouse model of diabetic nephropathy and its regression by bone morphogenic protein-7 and advanced glycation end product inhibitors.* Diabetes, 2007. **56**(7): p. 1825-33.
24. Zeisberg, M., M.A. Soubasakos, and R. Kalluri, *Animal models of renal fibrosis.* Methods Mol Med, 2005. **117**: p. 261-72.
25. Fink, M., M. Henry, and J.D. Tange, *Experimental folic acid nephropathy.* Pathology, 1987. **19**(2): p. 143-9.

26. Lim, B.J., H.C. Yang, and A.B. Fogo, *Animal models of regression/progression of kidney disease.* Drug Discov Today Dis Models, 2014. **11**: p. 45-51.
27. Rabe, M. and F. Schaefer, *Non-Transgenic Mouse Models of Kidney Disease.* Nephron, 2016. **133**(1): p. 53-61.
28. Eddy, A.A., et al., *Investigating mechanisms of chronic kidney disease in mouse models.* Pediatr Nephrol, 2012. **27**(8): p. 1233-47.
29. Lv, W., et al., *Inflammation and renal fibrosis: Recent developments on key signaling molecules as potential therapeutic targets.* Eur J Pharmacol, 2018. **820**: p. 65-76.
30. Black, L.M., J.M. Lever, and A. Agarwal, *Renal Inflammation and Fibrosis: A Double-edged Sword.* J Histochem Cytochem, 2019. **67**(9): p. 663-681.
31. Sheng, L. and S. Zhuang, *New Insights Into the Role and Mechanism of Partial Epithelial-Mesenchymal Transition in Kidney Fibrosis.* Front Physiol, 2020. **11**: p. 569322.
32. Miao, Z., et al., *Single cell regulatory landscape of the mouse kidney highlights cellular differentiation programs and disease targets.* Nat Commun, 2021. **12**(1): p. 2277.
33. Kuppe, C., et al., *Decoding myofibroblast origins in human kidney fibrosis.* Nature, 2021. **589**(7841): p. 281-286.
34. Jiang, B.H., et al., *Dimerization, DNA binding, and transactivation properties of hypoxia-inducible factor 1.* J Biol Chem, 1996. **271**(30): p. 17771-8.
35. Hu, C.J., et al., *The N-terminal transactivation domain confers target gene specificity of hypoxia-inducible factors HIF-1alpha and HIF-2alpha.* Mol Biol Cell, 2007. **18**(11): p. 4528-42.
36. Maxwell, P.H., et al., *The tumour suppressor protein VHL targets hypoxia-inducible factors for oxygen-dependent proteolysis.* Nature, 1999. **399**(6733): p. 271-5.
37. Schodel, J. and P.J. Ratcliffe, *Mechanisms of hypoxia signalling: new implications for nephrology.* Nat Rev Nephrol, 2019. **15**(10): p. 641-659.
38. Ziello, J.E., I.S. Jovin, and Y. Huang, *Hypoxia-Inducible Factor (HIF)-1 regulatory pathway and its potential for therapeutic intervention in malignancy and ischemia.* Yale J Biol Med, 2007. **80**(2): p. 51-60.
39. Dames, S.A., et al., *Structural basis for Hif-1 alpha /CBP recognition in the cellular hypoxic response.* Proc Natl Acad Sci U S A, 2002. **99**(8): p. 5271-6.
40. Majmundar, A.J., W.J. Wong, and M.C. Simon, *Hypoxia-inducible factors and the response to hypoxic stress.* Mol Cell, 2010. **40**(2): p. 294-309.
41. Geng, H., et al., *HIF1alpha protein stability is increased by acetylation at lysine 709.* J Biol Chem, 2012. **287**(42): p. 35496-35505.
42. Semenza, G.L., *Hypoxia-inducible factors in physiology and medicine.* Cell, 2012. **148**(3): p. 399-408.
43. Semenza, G.L. and G.L. Wang, *A nuclear factor induced by hypoxia via de novo protein synthesis binds to the human erythropoietin gene enhancer at a site required for transcriptional activation.* Mol Cell Biol, 1992. **12**(12): p. 5447-54.
44. Nakuluri, K., et al., *Cerebral ischemia induces TRPC6 via HIF1alpha/ZEB2 axis in the glomerular podocytes and contributes to proteinuria.* Sci Rep, 2019. **9**(1): p. 17897.
45. Lamouille, S., J. Xu, and R. Derynck, *Molecular mechanisms of epithelial-mesenchymal transition.* Nat Rev Mol Cell Biol, 2014. **15**(3): p. 178-96.
46. Lehtonen, S., et al., *CD2-associated protein is widely expressed and differentially regulated during embryonic development.* Differentiation, 2008. **76**(5): p. 506-17.
47. May, C.J., M. Saleem, and G.I. Welsh, *Podocyte dedifferentiation: a specialized process for a specialized cell.* Front Endocrinol (Lausanne), 2014. **5**: p. 148.

48. Petermann, A.T., et al., *Viable podocytes detach in experimental diabetic nephropathy: potential mechanism underlying glomerulosclerosis.* Nephron Exp Nephrol, 2004. **98**(4): p. e114-23.
49. Vogelmann, S.U., et al., *Urinary excretion of viable podocytes in health and renal disease.* Am J Physiol Renal Physiol, 2003. **285**(1): p. F40-8.
50. Nakuluri, K., et al., *Hypoxia induces ZEB2 in podocytes: Implications in the pathogenesis of proteinuria.* J Cell Physiol, 2019. **234**(5): p. 6503-6518.
51. Hung, T.W., et al., *Renal expression of hypoxia inducible factor-1alpha in patients with chronic kidney disease: a clinicopathologic study from nephrectomized kidneys.* Indian J Med Res, 2013. **137**(1): p. 102-10.
52. Reidy, K. and K. Susztak, *Epithelial-mesenchymal transition and podocyte loss in diabetic kidney disease.* Am J Kidney Dis, 2009. **54**(4): p. 590-3.
53. Higgins, D.F., et al., *Hypoxia promotes fibrogenesis in vivo via HIF-1 stimulation of epithelial-to-mesenchymal transition.* J Clin Invest, 2007. **117**(12): p. 3810-20.
54. Schell, C. and T.B. Huber, *The Evolving Complexity of the Podocyte Cytoskeleton.* J Am Soc Nephrol, 2017. **28**(11): p. 3166-3174.
55. Chang, J.M., et al., *B7-1 expression regulates the hypoxia-driven cytoskeleton rearrangement in glomerular podocytes.* Am J Physiol Renal Physiol, 2013. **304**(1): p. F127-36.
56. Endlich, N., F. Siegerist, and K. Endlich, *Are podocytes motile?* Pflugers Arch, 2017. **469**(7-8): p. 951-957.
57. Blaine, J. and J. Dylewski, *Regulation of the Actin Cytoskeleton in Podocytes.* Cells, 2020. **9**(7).
58. Salmon, A.H., et al., *Evidence for restriction of fluid and solute movement across the glomerular capillary wall by the subpodocyte space.* Am J Physiol Renal Physiol, 2007. **293**(6): p. F1777-86.
59. D'Agati, V., *And you thought the age of anatomic discovery was over.* J Am Soc Nephrol, 2005. **16**(5): p. 1166-8.
60. Pichler Sekulic, S. and M. Sekulic, *Rheological influence upon the glomerular podocyte and resultant mechanotransduction.* Kidney Blood Press Res, 2015. **40**(2): p. 176-87.
61. Brinkkoetter, P.T., et al., *Anaerobic Glycolysis Maintains the Glomerular Filtration Barrier Independent of Mitochondrial Metabolism and Dynamics.* Cell Rep, 2019. **27**(5): p. 1551-1566 e5.
62. Palm, F. and L. Nordquist, *Renal tubulointerstitial hypoxia: cause and consequence of kidney dysfunction.* Clin Exp Pharmacol Physiol, 2011. **38**(7): p. 474-80.
63. Kimura, K., et al., *Stable expression of HIF-1alpha in tubular epithelial cells promotes interstitial fibrosis.* Am J Physiol Renal Physiol, 2008. **295**(4): p. F1023-9.
64. Brukamp, K., et al., *Hypoxia and podocyte-specific Vhlh deletion confer risk of glomerular disease.* Am J Physiol Renal Physiol, 2007. **293**(4): p. F1397-407.
65. Nayak, B.K., et al., *HIF-1 Mediates Renal Fibrosis in OVE26 Type 1 Diabetic Mice.* Diabetes, 2016. **65**(5): p. 1387-97.
66. Baumann, B., et al., *Hypoxia-inducible factor-1alpha promotes glomerulosclerosis and regulates COL1A2 expression through interactions with Smad3.* Kidney Int, 2016. **90**(4): p. 797-808.
67. Schodel, J., et al., *Factor inhibiting HIF limits the expression of hypoxia-inducible genes in podocytes and distal tubular cells.* Kidney Int, 2010. **78**(9): p. 857-67.
68. Ji, T., et al., *TRPC6-Mediated Ca2+ Signaling is Required for Hypoxia-Induced Autophagy in Human Podocytes.* Cell Physiol Biochem, 2018. **48**(4): p. 1782-1792.

69. Olsen, K.C., et al., *Transglutaminase 2 and its role in pulmonary fibrosis.* Am J Respir Crit Care Med, 2011. **184**(6): p. 699-707.
70. Lorand, L. and R.M. Graham, *Transglutaminases: crosslinking enzymes with pleiotropic functions.* Nat Rev Mol Cell Biol, 2003. **4**(2): p. 140-56.
71. Lorand, L. and S.M. Conrad, *Transglutaminases.* Mol Cell Biochem, 1984. **58**(1-2): p. 9-35.
72. Lai, T.S. and C.S. Greenberg, *TGM2 and implications for human disease: role of alternative splicing.* Front Biosci (Landmark Ed), 2013. **18**: p. 504-19.
73. Jones, R.A., et al., *Matrix changes induced by transglutaminase 2 lead to inhibition of angiogenesis and tumor growth.* Cell Death Differ, 2006. **13**(9): p. 1442-53.
74. Facchiano, A. and F. Facchiano, *Transglutaminases and their substrates in biology and human diseases: 50 years of growing.* Amino Acids, 2009. **36**(4): p. 599-614.
75. Aeschlimann, D., D. Mosher, and M. Paulsson, *Tissue transglutaminase and factor XIII in cartilage and bone remodeling.* Semin Thromb Hemost, 1996. **22**(5): p. 437-43.
76. Keillor, J.W., K.Y. Apperley, and A. Akbar, *Inhibitors of tissue transglutaminase.* Trends Pharmacol Sci, 2015. **36**(1): p. 32-40.
77. Huang, L., et al., *Transglutaminase inhibition ameliorates experimental diabetic nephropathy.* Kidney Int, 2009. **76**(4): p. 383-94.
78. Liu, S., R.A. Cerione, and J. Clardy, *Structural basis for the guanine nucleotide-binding activity of tissue transglutaminase and its regulation of transamidation activity.* Proc Natl Acad Sci U S A, 2002. **99**(5): p. 2743-7.
79. Fesus, L. and M. Piacentini, *Transglutaminase 2: an enigmatic enzyme with diverse functions.* Trends Biochem Sci, 2002. **27**(10): p. 534-9.
80. Di Venere, A., et al., *Opposite effects of Ca(2+) and GTP binding on tissue transglutaminase tertiary structure.* J Biol Chem, 2000. **275**(6): p. 3915-21.
81. Eckert, R.L., et al., *Transglutaminase regulation of cell function.* Physiol Rev, 2014. **94**(2): p. 383-417.
82. Siegel, M. and C. Khosla, *Transglutaminase 2 inhibitors and their therapeutic role in disease states.* Pharmacol Ther, 2007. **115**(2): p. 232-45.
83. Leicht, D.T., et al., *TGM2: a cell surface marker in esophageal adenocarcinomas.* J Thorac Oncol, 2014. **9**(6): p. 872-81.
84. Mehta, K., J.Y. Fok, and L.S. Mangala, *Tissue transglutaminase: from biological glue to cell survival cues.* Front Biosci, 2006. **11**: p. 173-85.
85. Iismaa, S.E., et al., *GTP binding and signaling by Gh/transglutaminase II involves distinct residues in a unique GTP-binding pocket.* J Biol Chem, 2000. **275**(24): p. 18259-65.
86. Martinez-Salgado, C., A.B. Rodriguez-Pena, and J.M. Lopez-Novoa, *Involvement of small Ras GTPases and their effectors in chronic renal disease.* Cell Mol Life Sci, 2008. **65**(3): p. 477-92.
87. Jeitner, T.M., et al., *Mechanism for the inhibition of transglutaminase 2 by cystamine.* Biochem Pharmacol, 2005. **69**(6): p. 961-70.
88. Lorand, L., *DRPLA aggregation and transglutaminase, revisited.* Nat Genet, 1998. **20**(3): p. 231.
89. Lesort, M., et al., *Cystamine inhibits caspase activity. Implications for the treatment of polyglutamine disorders.* J Biol Chem, 2003. **278**(6): p. 3825-30.
90. Lai, T.S., et al., *Regulation of human tissue transglutaminase function by magnesium-nucleotide complexes. Identification of distinct binding sites for Mg-GTP and Mg-ATP.* J Biol Chem, 1998. **273**(3): p. 1776-81.
91. Aeschlimann, D. and M. Paulsson, *Transglutaminases: protein cross-linking enzymes in tissues and body fluids.* Thromb Haemost, 1994. **71**(4): p. 402-15.

92. Prat-Duran, J., et al., *Transglutaminase 2 as a novel target in chronic kidney disease - Methods, mechanisms and pharmacological inhibition.* Pharmacol Ther, 2021. **222**: p. 107787.
93. Griffin, M., L.L. Smith, and J. Wynne, *Changes in transglutaminase activity in an experimental model of pulmonary fibrosis induced by paraquat.* Br J Exp Pathol, 1979. **60**(6): p. 653-61.
94. Mirza, A., et al., *A role for tissue transglutaminase in hepatic injury and fibrogenesis, and its regulation by NF-kappaB.* Am J Physiol, 1997. **272**(2 Pt 1): p. G281-8.
95. Johnson, T.S., et al., *Transglutaminase inhibition reduces fibrosis and preserves function in experimental chronic kidney disease.* J Am Soc Nephrol, 2007. **18**(12): p. 3078-88.
96. Nakuluri, K., et al., *Stabilization of hypoxia-inducible factor 1alpha by cobalt chloride impairs podocyte morphology and slit-diaphragm function.* J Cell Biochem, 2018.
97. Nishad, R., et al., *Growth hormone induces mitotic catastrophe of glomerular podocytes and contributes to proteinuria.* Cell Death Dis, 2021. **12**(4): p. 342.
98. Mungamuri, S.K., et al., *Ash2L enables P53-dependent apoptosis by favoring stable transcription pre-initiation complex formation on its pro-apoptotic target promoters.* Oncogene, 2015. **34**(19): p. 2461-70.
99. Diaz-Villasenor, A., et al., *Arsenite reduces insulin secretion in rat pancreatic beta-cells by decreasing the calcium-dependent calpain-10 proteolysis of SNAP-25.* Toxicol Appl Pharmacol, 2008. **231**(3): p. 291-9.
100. J.E. Folk, P.W.C., *Transglutaminase: Mechanistic features of the active site as determined by kinetic and inhibitor studies.* Biochimica et Biophysica Acta (BBA), 1996. **122**(2): p. 244-264.
101. Hart, P.C., et al., *Mesothelial Cell HIF1alpha Expression Is Metabolically Downregulated by Metformin to Prevent Oncogenic Tumor-Stromal Crosstalk.* Cell Rep, 2019. **29**(12): p. 4086-4098 e6.
102. Ye, J., et al., *Metformin suppresses hypoxiainduced migration via the HIF1alpha/VEGF pathway in gallbladder cancer in vitro and in vivo.* Oncol Rep, 2018. **40**(6): p. 3501-3510.
103. Singh, A.K., et al., *Detrimental effects of hypoxia on glomerular podocytes.* J Physiol Biochem, 2021. **77**(2): p. 193-203.
104. Kumar, A., et al., *Evidence that aberrant expression of tissue transglutaminase promotes stem cell characteristics in mammary epithelial cells.* PLoS One, 2011. **6**(6): p. e20701.
105. Kumar, A., et al., *Tissue transglutaminase promotes drug resistance and invasion by inducing mesenchymal transition in mammary epithelial cells.* PLoS One, 2010. **5**(10): p. e13390.
106. Kumar, S. and K. Mehta, *Tissue transglutaminase constitutively activates HIF-1alpha promoter and nuclear factor-kappaB via a non-canonical pathway.* PLoS One, 2012. **7**(11): p. e49321.
107. Jang, G.Y., et al., *Transglutaminase 2 suppresses apoptosis by modulating caspase 3 and NF-kappaB activity in hypoxic tumor cells.* Oncogene, 2010. **29**(3): p. 356-67.
108. Mann, A.P., et al., *Overexpression of tissue transglutaminase leads to constitutive activation of nuclear factor-kappaB in cancer cells: delineation of a novel pathway.* Cancer Res, 2006. **66**(17): p. 8788-95.
109. Yamaguchi, H. and H.G. Wang, *Tissue transglutaminase serves as an inhibitor of apoptosis by cross-linking caspase 3 in thapsigargin-treated cells.* Mol Cell Biol,

2006. **26**(2): p. 569-79.
110. Park, K.S., et al., *Depletion of nucleophosmin via transglutaminase 2 cross-linking increases drug resistance in cancer cells.* Cancer Lett, 2009. **274**(2): p. 201-7.
111. Cho, S.Y., et al., *Transglutaminase 2 mediates hypoxia-induced selective mRNA translation via polyamination of 4EBPs.* Life Sci Alliance, 2020. **3**(3).
112. Baandrup, J.D., et al., *Pressure load: the main factor for altered gene expression in right ventricular hypertrophy in chronic hypoxic rats.* PLoS One, 2011. **6**(1): p. e15859.
113. DiRaimondo, T.R., et al., *Elevated transglutaminase 2 activity is associated with hypoxia-induced experimental pulmonary hypertension in mice.* ACS Chem Biol, 2014. **9**(1): p. 266-75.
114. Rasouly, H.M., et al., *Loss of Zeb2 in mesenchyme-derived nephrons causes primary glomerulocystic disease.* Kidney Int, 2016. **90**(6): p. 1262-1273.
115. Kumar, P.A., et al., *Growth hormone (GH)-dependent expression of a natural antisense transcript induces zinc finger E-box-binding homeobox 2 (ZEB2) in the glomerular podocyte: a novel action of gh with implications for the pathogenesis of diabetic nephropathy.* J Biol Chem, 2010. **285**(41): p. 31148-56.
116. Chitra, P.S., et al., *Growth Hormone Induces Transforming Growth Factor-Beta-Induced Protein in Podocytes: Implications for Podocyte Depletion and Proteinuria.* J Cell Biochem, 2015. **116**(9): p. 1947-56.
117. Ahmed, A.A., et al., *The extracellular matrix protein TGFBI induces microtubule stabilization and sensitizes ovarian cancers to paclitaxel.* Cancer Cell, 2007. **12**(6): p. 514-27.
118. Farmer, L.K., et al., *TRPC6 Binds to and Activates Calpain, Independent of Its Channel Activity, and Regulates Podocyte Cytoskeleton, Cell Adhesion, and Motility.* J Am Soc Nephrol, 2019. **30**(10): p. 1910-1924.
119. Case, A. and R.L. Stein, *Kinetic analysis of the interaction of tissue transglutaminase with a nonpeptidic slow-binding inhibitor.* Biochemistry, 2007. **46**(4): p. 1106-15.
120. Duval, E., et al., *Structure-activity relationship study of novel tissue transglutaminase inhibitors.* Bioorg Med Chem Lett, 2005. **15**(7): p. 1885-9.
121. Calzavacca, P., et al., *Long-term measurement of renal cortical and medullary tissue oxygenation and perfusion in unanesthetized sheep.* Am J Physiol Regul Integr Comp Physiol, 2015. **308**(10): p. R832-9.
122. Hirakawa, Y., T. Tanaka, and M. Nangaku, *Renal Hypoxia in CKD; Pathophysiology and Detecting Methods.* Front Physiol, 2017. **8**: p. 99.
123. Vinovskis, C., et al., *Relative Hypoxia and Early Diabetic Kidney Disease in Type 1 Diabetes.* Diabetes, 2020. **69**(12): p. 2700-2708.
124. Faivre, A., C.C. Scholz, and S. de Seigneux, *Hypoxia in chronic kidney disease: towards a paradigm shift?* Nephrol Dial Transplant, 2020.
125. Provenzano, R., et al., *Oral Hypoxia-Inducible Factor Prolyl Hydroxylase Inhibitor Roxadustat (FG-4592) for Treatment of Anemia in Chronic Kidney Disease: A Placebo-Controlled Study of Pharmacokinetic and Pharmacodynamic Profiles in Hemodialysis Patients.* J Clin Pharmacol, 2020. **60**(11): p. 1432-1440.

ZEB2/TRPC6 axis transduce HIF1α dependent regulation of Transglutaminase 2 in glomerular podocytes

Lakshmi P Kolligundla, Ashish K Singh, Rajesh Kavvuri, Anil K Pasupulati.

Department of Biochemistry, School of Life Sciences, University of Hyderabad, Hyderabad, India.

Keywords: Podocytes; HIF1α; ZEB2; TRPC6; Transglutaminase 2; Fibrosis; Proteinuria

Correspondence to: F73B, Department of Biochemistry, School of Life Sciences, University of Hyderabad, Gachibowli, Hyderabad- 500046, India; Email: pasupulati.anilkumar@gmail.com (AKP).

Journal of Physiology and Biochemistry (2021) 77:193–203
https://doi.org/10.1007/s13105-021-00788-y

REVIEW

Detrimental effects of hypoxia on glomerular podocytes

Ashish K. Singh[1] · Lakshmi P. Kolligundla[1] · Justus Francis[1] · Anil K. Pasupulati[1]

Received: 5 August 2020 / Accepted: 11 January 2021 / Published online: 9 April 2021

Abstract

Hypoxia-inducible factor1 (HIF1) plays a pivotal role in ensuring cells adapt to low-oxygen conditions. Depletion of oxygen, a co-substrate during hydroxylation of prolyl (P402 and P564) residues of HIF1α, evades HIF1α ubiquitination and enables its dimerization with HIF1β to mediate global transcriptional response to hypoxia. Though HIF1 is largely considered eliciting a protective role during physiological or pathological hypoxia or ischemia, elevated HIF1 during chronic hypoxia contributes to glomerular diseases' pathology and proteinuria. The glomerulus is responsible for renal permselectivity and excretion of ultra-filtrated urine. Podocytes are the glomerulus' major cell types and are instrumental for glomerular filtration, permselectivity, and glomerular basement membrane maintenance. Podocyte injury is expected to impair the efficiency of glomerular filtration and manifestation of glomerulosclerosis and proteinuria. Accumulated evidence suggests that podocytes are susceptible to various insults during chronic hypoxia, including podocyte EMT, slit-diaphragm dysfunction, foot process effacement, and cytoskeletal derangement due to accumulation of HIF1. This review discusses how hypoxia/HIF1 signaling regulates various features and function of podocytes during exposure to chronic hypoxia or inducing HIF1 by various chemical modulators.

Keywords Hypoxia · HIF · Podocyte · EMT · Slit-diaphragm · Proteinuria

Abbreviations

CKD	Chronic kidney disease
EMT	Epithelial-to-mesenchymal transition
EPO	Erythropoietin
ESRD	End-stage renal disease
GBM	Glomerular basement membrane
GFB	Glomerular filtration barrier
HIF	Hypoxia-inducible factor
MET	Mesenchymal to epithelial transdifferentiation
PHD	Prolyl hydroxylase
PKD	Polycystic kidney disease
SD	Slit-diaphragm

Key Points • Podocytes, which regulate glomerular permselectivity, are susceptible to hypoxic injury.
• Accumulation of HIF1α results in epithelial-mesenchymal transition of podocytes.
• HIF1α suppresses podocyte slit-diaphragm proteins and thus impairs their permselectivity.
• Podocyte compromises their shape due to cytoskeletal deformities induced by HIF1α.

Ashish K. Singh and Lakshmi P. Kolligundla contributed equally to this work.

✉ Anil K. Pasupulati
pasupulati.anilkumar@gmail.com

[1] Department of Biochemistry, School of Life Sciences, University of Hyderabad, Hyderabad, India

Introduction

Kidneys regulate several functions, including erythropoiesis, electrolyte, water, and acid–base balance, and are thus indispensable in ensuring the body's homeostasis. Human kidneys elicit these functions with the collective effort of ~ 2.0 million nephrons [27]. Nephron, the functional unit of the kidney, consists of two regions: glomerulus and tubule. The glomerulus is responsible for filtering water and small molecules from the blood to form primary urine. Whereas the tubular system ensures selective reabsorption and secretion, thus fine-tune the final composition of urine. Under normal conditions, kidneys help excrete ultra-filtrated urine with a tightly regulated composition [1].

Urinary excretion of albumin at varying degrees is a well-known predictor of renal outcome [2]. Microalbuminuria (30 to 300 mg/24 h) followed by macroalbuminuria (≥ 300 mg/24 h) over months to years indicate progressive renal function loss. Proteinuria for an extended period is

SCIENTIFIC REPORTS
nature research

OPEN

Cerebral ischemia induces TRPC6 via HIF1α/ZEB2 axis in the glomerular podocytes and contributes to proteinuria

Krishnamurthy Nakuluri[1,5], Rajkishor Nishad[1,5], Dhanunjay Mukhi[1], Sireesh Kumar[2], Venkata P. Nakka[3], Lakshmi P. Kolligundla[1], Parimala Narne[2], Sai Sampath K. Natuva[4], Prakash Babu Phanithi[2*] & Anil K. Pasupulati[1*]

Podocytes are specialized cells of the glomerulus and key component of the glomerular filtration apparatus (GFA). GFA regulates the permselectivity and ultrafiltration of blood. The mechanism by which the integrity of the GFA is compromised and manifest in proteinuria during ischemic stroke remains enigmatic. We investigated the mechanism of ischemic hypoxia-induced proteinuria in a middle cerebral artery occlusion (MCAO) model. Ischemic hypoxia resulted in the accumulation of HIF1α in the podocytes that resulted in the increased expression of ZEB2 (Zinc finger E-box-binding homeobox 2). ZEB2, in turn, induced TRPC6 (transient receptor potential cation channel, subfamily C, member 6), which has increased selectivity for calcium. Elevated expression of TRPC6 elicited increased calcium influx and aberrant activation of focal adhesion kinase (FAK) in podocytes. FAK activation resulted in the stress fibers reorganization and podocyte foot process effacement. Our study suggests overactive HIF1α/ZEB2 axis during ischemic-hypoxia raises intracellular calcium levels via TRPC6 and consequently altered podocyte structure and function thus contributes to proteinuria.

Extreme physiological and pathological conditions impose challenges on human physiology. The normal functioning of the human body demands both continuous and adequate supply of oxygen whereas relative (hypoxia) and the absolute deficiency (anoxia) of oxygen are a risk to human health. Human organs vary in their oxygen dependency and susceptibility to oxygen deficiency. Brain and kidney are most hypoxia-sensitive organs. Oxygen is involved in the formation of ATP from ADP and ATP-dependent active salt reabsorption in kidney demands high oxygen supply[1]. Kidney carries out its functions within a narrow range of partial pressure of oxygen, which is very low in the inner medulla (5 mmHg) compared with the outer cortex (50 mmHg)[2]. Furthermore, renal vasculature despite its low-resistance subjected to continuous perfusion[3,4]. Vascular architecture of the kidney and surplus demand for oxygen together let the kidneys highly sensitive to oxygen-deprived conditions[1,5,6]. Limitations in oxygen supply impose kidneys to undergo hypoxia-induced maladaptation, which likely reflects in the pathophysiology of acute kidney injury and proteinuria[6–12].

The vertebrate kidneys regulate homeostasis predominantly by controlling acid-base, electrolyte, and water balance. Kidneys are also instrumental in ultrafiltration of plasma components and regulating the composition of urine. Proteinuric condition suggests abnormalities in the glomerular filtration apparatus (GFA)[13]. Three layers of GFA are podocytes, glomerular basement membrane (GBM), and perforated endothelium[13]. Clinical conditions such as stroke and sleep apnea are associated with proteinuria and are presented with reduced renal perfusion and moderate to severe hypoxia[12,14]. Accumulated evidence suggests that hypoxia contributes to the proteinuria and pathogenesis of chronic kidney disease (CKD)[6,7,10,15–17]. The prevalence of CKD is more than 30% among stroke subjects[18]. Renal dysfunction is a worse clinical outcome in patients with ischemic stroke[19,20] and it is an independent predictor of stroke mortality[18].

[1]Department of Biochemistry, University of Hyderabad, Hyderabad, 500046, India. [2]Department of Biotechnology & Bioinformatics, University of Hyderabad, Hyderabad, 500046, India. [3]Department of Biochemistry, Acharya Nagarjuna University, Guntur, 522510, India. [4]Narayana Medical College, Nellore, 524003, India. [5]These authors contributed equally: Krishnamurthy Nakuluri and Rajkishor Nishad. *email: prakash@uohyd.ac.in; pasupulati.anilkumar@gmail.com

Research Communication

In Silico Structural Characterization of Podocin and Assessment of Nephrotic Syndrome-Associated Podocin Mutants

Sandeep Kumar
Narasimha Mulukala[1]
Rajkishor Nishad[1]
Lakshmi Prasanna Kolligundla[1]
Moin A. Saleem[2]
Nagu Prakash Prabhu[3]
Anil Kumar Pasupulati[1]*

[1]*Department of Biochemistry, School of Life Sciences, University of Hyderabad, Hyderabad, Telangana, India*
[2]*Academic Renal Unit, School of Clinical Sciences, University of Bristol, Bristol, United Kingdom*
[3]*Department of Biotechnology and Bioinformatics, University of Hyderabad, Hyderabad, Telangana, India*

Abstract

Nephrotic syndrome (NS) is manifested by hyperproteinuria, hypoalbuminemia, and edema. *NPHS2* that encodes podocin was found to have most mutations among the genes that are involved in the pathophysiology of NS. Podocin, an integral membrane protein belonging to stomatin family, is expressed exclusively in podocytes and is localized to slit-diaphragm (SD). Mutations in podocin are known to be associated with steroid-resistant NS and rapid progression to end-stage renal disease, thus signifying its role in maintaining SD integrity and podocyte function. The structural insights of podocin are not known, and the precise mechanism by which podocin contributes to the architecture of SD is yet to be elucidated. In this study, we deduced a model for human podocin, discussed the details of transmembrane localization and intrinsically unstructured regions, and provide an understanding of how podocin interacts with other SD components. Intraprotein interactions were assessed in wild-type podocin and in some of its mutants that are associated with idiopathic NS. Mutations in podocin alter the innate intraprotein interactions affecting the native structure of podocin and its ability to form critical complex with subpodocyte proteins. © 2016 IUBMB Life, 68(7):578–588, 2016

Keywords: *nephrotic syndrome; proteinuria; podocytes; podocin; slit diaphragm; molecular modeling*

Introduction

The kidneys are vital organs that help to maintain body homeostasis by regulating blood pressure, acid–base, electrolyte, and water balance. Human kidney constitutes a million nephrons that collectively perform three key events including (*a*) glomerular filtration of water and small molecules from renal plasma; (*b*) tubular reabsorption of glomerular filtrate; and (*c*) tubular secretion of metabolic waste products into the filtrate. Thus, glomerulus in concert with tubular region of the nephron tightly regulates the composition of glomerular filtrate and ensures almost protein-free ultrafiltrated urine. Glomerulus, where initiation of filtration occurs, contains a tuft of capillaries and several resident cell types that include mesangial cells, endothelial cells, and glomerular visceral epithelial cells, also known as podocytes.

Proteinuria is a hallmark of renal damage in several glomerular diseases due to the alterations in glomerular filtration barrier (GFB; refs. 1 and 2). The three components that constitute GFB include fenestrated glomerular endothelial cells, glomerular basement membrane (GBM), and glomerular visceral epithelial cells, known as podocytes. A wealth of literature highlighted that podocytes are critical for glomerular filtration (3,4). Podocytes are terminally differentiated epithelial cells

Volume 68, Number 7, July 2016, Pages 578–588
**Address correspondence to: Anil Kumar Pasupulati, Department of Biochemistry, School of Life Sciences, University of Hyderabad, Gachibowli, Hyderabad 500046, Andhra Pradesh, India.*
Tel: +91-40-23134519. Fax: +91-40-23010120.
E-mail: pasupulati.anilkumar@gmail.com
Received 14 April 2016; Accepted 3 May 2016
DOI 10.1002/iub.1515
Published online 18 May 2016 in Wiley Online Library (wileyonlinelibrary.com)

Identification of Potent Reversible Inhibitors for Transglutaminase 2

Lakshmi P Kolligundla, Samriddhi Gupta, Sandeep KN Mulukala*, Anil K Pasupulati*

Department of Biochemistry, School of Life Sciences, University of Hyderabad, Hyderabad, India.

Short-title: Screening inhibitors for Tissue transglutaminase

Keywords: Transglutaminase 2, fibrosis, inhibitor, GTP

*Correspondence to**:** SKNM (sandeep2k9@yahoo.com) & AKP (anilkumar@uohyd.ac.in), F73B, School of Life Sciences, University of Hyderabad, Gachibowli, Hyderabad-500046, India.

International Conference and Workshop

On

IIITH

Structure-based Drug Designing and Applications to Infectious Diseases

1st - 5th February, 2016

Participation Certificate

This is to certify that K. LAKSHMI PRASANNA has participated and presented POSTER in the International Conference and Workshop of "Structure-based Drug Designing and Applications to Infectious Diseases" during the period 1st - 5th February, 2016, University of Hyderabad & IIITH, Hyderabad.

SBDD 2016 UNIVERSITY OF HYDERABAD

Organizers

NWMDSDD 2019

DEPARTMENT OF ZOOLOGY - KAKATIYA UNIVERSITY

Accredited with "A" Grade by NAAC

Vidyaranyapuri, WARANGAL-506009, Telangana - INDIA

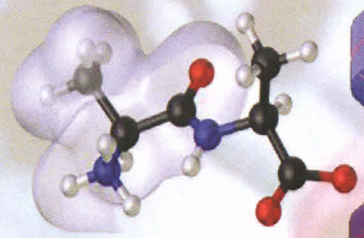

National Workshop on

MOLECULAR DOCKING STUDIES IN DRUG DISCOVERY

CERTIFICATE

This is to certify that ..... Kolligundla Lakshmi Prasanna .....
has participated and successfully completed the National Workshop on "Molecular Docking Studies in Drug Discovery", organized by the Department of Zoology, Kakatiya University, Warangal from 29-31st May, 2019.

Director:
Dr. E. Narayana

Convener:
Dr. G. Shamitha

Organising Secretary:
Dr. Estari Mamidala

PE - 33

85th Annual Meeting of Society of Biological Chemists (India)

CSIR-Central Food Technological Research Institute, Mysuru, INDIA

21st - 24th November 2016

POSTER PRESENTATION CERTIFICATE

This is to certify that Dr./Mr./Ms. AK Pasupulati1, **Lakshmi Prasanna K**, Arpita Devi and Aramati BM Reddy

has participated and presented his/her research findings entitled **Inhibitors for tissue transglutaminase: a potential drug target to combat renal fibrosis.** *in the scientific session as poster presentation in the "85th Annual Meeting of Society of Biological Chemists (India)" held during 21st to 24th November, 2016 at CSIR-Central Food Technological Research Institute, Mysuru, INDIA.*

Dr. Alok K. Srivastava
Chief Scientist, CSIR-CFTRI
Chairman, Poster Committee
SBC(I) Meet - 2016

Prof. Ram Rajasekharan
Director, CSIR-CFTRI
Chairman, Local Organizing Committee
SBC(I) Meet - 2016

School of Life Sciences
University of Hyderabad

GLOBAL INITIATIVE OF ACADEMIC NETWORKS

Cornell University
USA

सत्यमेव जयते
Ministry of
Human Resource Development
Government of India

Global Initiative on Academic Networks

Immunologicals in Animal and Human Health

Certificate of Participation

This is to certify that Prof. / Dr. / Mr. / Ms. Lakshmi Prasanna K

from **UoH, Hyderabad** participated in the course titled **"Immunologicals in Animal and Human Health"** during the period from **July 04 - 16, 2016**, School of Life Sciences, University of Hyderabad, Hyderabad, INDIA.

Dr. Pallu Reddanna
Dean, School of Life Sciences

Dr. Nirmal Viswanathan
GIAN, Local Coordinator

Dr. Avery August
Course Coordinator

Dr. Aramati BM Reddy
Course Coordinator

Research Methodology Workshop Series-4
Literature review and Data analysis using SPSS
26-27th of February, 2019 at School of Medical Sciences,
University of Hyderabad

CERTIFICATE

This is to certify that Dr./Mr./Ms./Shri. K. Lakshmi Prasanna
participated in the Research
Methodology Workshop Series-4 Literature review and Data Analysis using SPSS conducted by School of Medical Sciences, University of Hyderabad.

ORGANIZER
SCHOOL OF MEDICAL SCIENCES

DEAN,
SCHOOL OF MEDICAL SCIENCES

BioQuest 2015

23rd - 24th September

School of Life Sciences
University of Hyderabad
Hyderabad - 500 046, INDIA

Certificate of Participation

This is to certify that Prof./Dr./Mr./Ms. KOLLI GUNDLA LAKSHMI PRASANNA

from Department of Biochemistry

has participated in the *"BioQuest 2015"* held on September 23rd and 24th, 2015.

Convener

Dean
School of Life Sciences

BioQUEST

12th & 13th October, 2017

School of Life Sciences
University of Hyderabad
Hyderabad – 500 046, INDIA

Certificate of Presentation

This is to certify that Prof./Dr./Mr./Ms./Mrs. Lakshmi Prasanna K.

from department of Biochemistry has participated

and made oral/poster presentation entitled _____

_____ in BioQuest-2017 held on 12 and 13

October, 2017 at School of Life Sciences, University of Hyderabad.

Dean
School of Life Sciences

USE OF RADIATION TECHNOLOGY IN AGRICULTURE, HEALTH AND REASEARCH

UNIVERSITY OF HYDERABAD - BHABHA ATOMIC RESEARCH CENTER

SCHOOL OF LIFE SCIENCES

UNIVERSITY OF HYDERABAD - 500046

SCHOOL OF LIFE SCIENCES

Certificate of Participation

This is to certify that Dr./Mr./Ms .....K. Lakshmi Prasanna.....

from .....Dept. of Biochemistry, UoH..... has participated in a one day national seminar

on "THE USE OF RADIATION TECHNOLOGY" conducted by The University of Hyderabad

and Bhabha Atomic Research Center on 13th November, 2015.

P. Anil Kumar

Organising Secretary

Department of Biochemistry

School of Life Sciences

Studies on Regulation of Transglutaminase 2 in Hypoxia-induced Chronic Kidney Disease

by Lakshmi Prasanna Kolligundla

Submission date: 11-Aug-2021 12:48PM (UTC+0530)
Submission ID: 1630203188
File name: Lakshmi_Prasanna_Kolligundla.docx (274.76K)
Word count: 12685
Character count: 75200

P. Al Kumar

Dr. P. ANIL KUMAR
Assistant Professor
Department of Biochemistry
University of Hyderabad
Hyderabad-500 046, India.

Studies on Regulation of Transglutaminase 2 in Hypoxia-induced Chronic Kidney Disease

ORIGINALITY REPORT

17%	4%	17%	2%
SIMILARITY INDEX	INTERNET SOURCES	PUBLICATIONS	STUDENT PAPERS

PRIMARY SOURCES

1	Ashish K. Singh, Lakshmi P. Kolligundla, Justus Francis, Anil K. Pasupulati. "Detrimental effects of hypoxia on glomerular podocytes", Journal of Physiology and Biochemistry, 2021 Publication	12%
2	hdl.handle.net Internet Source	1%
3	M SIEGEL, C KHOSLA. "Transglutaminase 2 inhibitors and their therapeutic role in disease states", Pharmacology & Therapeutics, 2007 Publication	<1%
4	Rajkishor Nishad, Dhanunjay Mukhi, Ashish Kumar Singh, Kumaraswami Chintala, Prasad Tammineni, Anil Kumar Pasupulati. "Growth hormone induces mitotic catastrophe of podocytes and contributes to proteinuria", Cold Spring Harbor Laboratory, 2020 Publication	<1%
5	Krishnamurthy Nakuluri, Rajkishor Nishad, Dhanunjay Mukhi, Sireesh Kumar et al.	<1%

This manuscript is authored (& Equal first) by Ms. Lakshmi Prasanna Therefore 12% of similarity may be exempted from 17%.
P. Anil Kumar

Dr. P. ANIL KUMAR
Assistant Professor
Department of Biochemistry
University of Hyderabad
Hyderabad-500 046. India.

P. Anil Kumar

Dr. P. ANIL KUMAR
Assistant Professor
Department of Biochemistry
University of Hyderabad
Hyderabad-500 046. India.